Missing the sweet spot: one of the two N-glycans on human Gb3/CD77 synthase curtails its activity

Krzysztof Mikolajczyk[1], Anna Bereznicka[1], Katarzyna Szymczak-Kulus[1], Katarzyna Haczkiewicz- Lesniak[2], Bozena Szulc[3], Mariusz Olczak[3], Joanna Rossowska[4], Edyta Majorczyk[5], Katarzyna Kapczynska[6], Nicolai Bovin[7], Marta Lisowska[8], Radoslaw Kaczmarek[1], Arkadiusz Miazek[8], Marcin Czerwinski*[1]

[1] Laboratory of Glycobiology, Hirszfeld Institute of Immunology and Experimental Therapy, Polish Academy of Sciences, Weigla St. 12, 53-114 Wroclaw, Poland.
[2] Division of Ultrastructure Research, Wroclaw Medical University, Chalubinskiego St. 6a, 50-368 Wroclaw, Poland.
[3] Faculty of Biotechnology, University of Wroclaw, 14A F. Joliot-Curie St., 50-383 Wroclaw, Poland.
[4] Flow Cytometry Core Facility, Hirszfeld Institute of Immunology and Experimental Therapy, Polish Academy of Sciences, Weigla St. 12, 53-114 Wroclaw, Poland.
[5] Faculty of Physiotherapy and Physical Education, Opole University of Technology, 76 Proszkowska St., 45-758 Opole, Poland.
[6] Department of Immunology of Infectious Diseases, Hirszfeld Institute of Immunology and Experimental Therapy, Polish Academy of Sciences, Weigla St. 12, 53-114 Wroclaw, Poland.
[7] Shemyakin-Ovchinnikov Institute of Bioorganic Chemistry Russian Academy of Sciences, 16/10 Miklukho-Maklaya str. Moscow 117997 Russia.
[8] Department of Tumor Immunology, Hirszfeld Institute of Immunology and Experimental Therapy, Polish Academy of Sciences, Weigla St. 12, 53-114 Wroclaw, Poland.

*Corresponding author: Marcin Czerwinski

E-mail: marcin.czerwinski@hirszfeld.pl

Keywords: glycosphingolipid, glycosyltransferase, A4GALT, activity, Shiga toxin

Abstract

N-glycosylation is a ubiquitous posttranslational modification that may influence folding, subcellular localization, secretion, solubility and oligomerization of proteins. In this study, we examined the role of N-glycans in the activity of human Gb3/CD77 synthase, which catalyzes the synthesis of glycosphingolipids with terminal Galα1→4Galβ (Gb3 and the P1 antigen) and Galα1→4GalNAcβ disaccharides (the NOR antigen). The human Gb3/CD77 synthase contains two occupied N-glycosylation sites at positions N_{121} and N_{203}. Intriguingly, we found that while the N-glycan at N_{203} is essential for activity and correct subcellular localization, the N-glycan at N_{121} is dispensable and a glycoform without it showed increased enzyme activity. The fully N-glycosylated human Gb3/CD77 synthase and its glycoform missing the N_{121} glycan correctly localize in the Golgi, whereas a glycoform without the N_{203} site partially mislocalized in the endoplasmic reticulum. A double mutein missing both N-glycans was inactive and accumulated in the ER. Our results suggest that the decreased specific activity of human Gb3/CD77 synthase glycovariants results from their improper subcellular localization and, to a smaller degree, a decrease in enzyme solubility. Taken together, our findings show that the two N-glycans of human Gb3/CD77 synthase have opposing effects on its properties, revealing a dual nature of N-glycosylation and potentially a novel regulatory mechanism controlling biological activity of proteins.

Introduction

Glycosyltransferases (GTs) constitute a large group of enzymes catalyzing transfer of sugar residues from carbohydrate donors (*e.g.* UDP-Gal, CMP-NeuNAc) to diverse acceptor molecules, forming glycosidic bonds with retention or inversion of the attached sugar configuration [Breton C., Fournel-Gigleux S. et al. 2012]. On the basis of structural analysis most GTs are classified into five overall folds: GT-A [Taujale R., Venkat A. et al. 2020], GT-B [Albesa-Jové D., Giganti D. et al. 2014], GT-C [Bohl T., Bai L. et al 2021], GT-D [Zhang H., Zhou M. et al. 2016] and GT-E [Kattke M.D., Gosschalk J.E. et al. 2019].

N-glycosylation is a ubiquitous posttranslational modification (PTM) of proteins; an estimated 70% may be N-glycosylated [Gavel Y., von Heijne G. et al. 1990]. N-glycans are attached to a protein by asparagine within a canonical N-X-S/T motif called sequon (where X is any amino acid residue except proline); however, other sequons, such as N-X-C, N-Q-C, N-S-G or Q-G-T sequons (referred to as noncanonical) may also be utilized [Lowenthal M.S., Davis K.S. et al. 2016]. In eukaryotes, biosynthesis of N-glycans occurs in two cellular compartments: (1) the endoplasmic reticulum (ER) in which the dolichol-P-linked oligosaccharide substrate is attached to an asparagine, and (2) the Golgi apparatus, which contains glycan-processing enzymes involved in trimming and maturation of N-glycans [Stanley P., Taniguchi N. et al. 2017]. Glycosylation may play a major role in many cellular processes, such as protein folding [Jayaprakash N.G., Surolia A. et al. 2017], maturation [Agthe M., Garbers Y. et al. 2018], secretion [Fiedler K., Simons K. et al. 1995], intracellular trafficking [Rosnoblet C., Peanne R. et al. 2013], cell-cell interactions [Varki A., 2017], immune responses [Ryan S.O., Cobb B.A. et al. 2012] and disease progression [Kizuka Y., Kitazume S. et al. 2017; Vajaria B.N., Patel P.S. et al. 2017].

Human Gb3/CD77 synthase (α1,4-galactosyltransferase, P1/P^k synthase, EC 2.4.1.228) encoded by the *A4GALT* gene, is a type II transmembrane GT with C-terminal globular catalytic domain and N-termini domain contained transmembrane domain; it belonging to the glycosyltransferase family 32. The enzyme retains the anomeric carbon stereochemistry after glycosidic bond formation [Furukawa K., Kondo Y. et al. 2014; Okuda T., Tokuda N. et al. 2006]. *In silico* analysis predicted the GT-A fold type (Carbohydrate Active Enzymes database, http://www.cazy.org/). Members of the GT-A superfamily require a divalent metal ion (usually Mn^{2+}) at the catalytic center, which is coordinated by two aspartic acid residues, creating a DXD motif (D_{192}TD in human Gb3/CD77 synthase according to UniProt Q9NPC4, https://www.uniprot.org/).

Previously, we found that in addition to the high-frequency *A4GALT* gene variant (GenBank NG_007495.2), there is another one with a point mutation c.631C>G (rs397514502, GenBank NG_007495.2) giving rise to the protein with p.Q211E substitution (hereafter referred to as E or mutein). The enzyme (here designated as Q) encoded by the high-frequency gene catalyzes the transfer of galactose from UDP-galactose to lactosylceramide or paragloboside, producing globotriaosylceramide (Gb3, P^k, CD77) and P1 antigen, respectively. Both Gb3 and P1 are terminated with Galα1→4Gal moiety. It was recently shown that Gb3/CD77 synthase can add galactose also to Galβ1-Cer, creating galabiosylceramide (Galα1-4Galβ1-Cer) [Akiyama H., Ide M. et al. 2021]. The mutein transfers galactose residue additionally to a terminal GalNAc, giving rise to the rare NOR antigen (carried by NOR1, NOR_{int} and NOR2 glycosphingolipids), which terminate with Galα1→4GalNAcβ structures [Suchanowska A., Kaczmarek R. et al. 2012]. The ability of human Gb3/CD77 synthase to utilize two different carbohydrate moieties on acceptors is a unique case of glycosyltransferase promiscuity, breaking the old 'one enzyme-one linkage' tenet [Kaczmarek R., Duk M. et al. 2016]. All these antigens (Gb3, P1 and NOR) belong to the human P1PK blood group system: the presence or absence of P1 on red blood cells (RBCs) determines the P_1 or P_2 blood group phenotypes, respectively. In the rare p phenotype, which may be caused by null mutations in *A4GALT*, the P1PK antigens are not detected on RBCs. Presence of the NOR antigens results in the rare NOR phenotype [Kaczmarek R., Szymczak-Kulus K. et al. 2018; Kaczmarek R., Buczkowska A. et al. 2014].

Gb3 is present in human RBCs and lymphocytes, heart, lung, kidney, smooth muscle and epithelium of gastrointestinal tract [Cooling L., 2015]. Several reports showed that elevated expression of Gb3 was found in colorectal, gastric and ovarian cancers [Kovbasnjuk O., Mourtazina R. et al. 2005; Geyer P.E., Maak M. et al. 2016]. In Fabry's disease, which is an X-linked lysosomal storage disorder caused by deficiency of α-galactosidase (OMIM 301500), Gb3 accumulates in organs throughout the body [Miller J.J., Kanack A.J. et al. 2020]. Expression of P1 antigen seems to be limited to the erythroid lineage [Cooling L., 2015], but it was also detected on ovarian cancer cells, where it was designated a cancer-associated antigen [Jacob F., Anugraham M. et al. 2014].

Galα1→4Galβ disaccharide-containing glycosphingolipids (GSLs), such as Gb3 are targeted by bacterial adhesins, including PapG of uropathogenic *Escherichia coli*, and viruses [Cooling L., 2015]. Gb3 is also the main receptor for Shiga toxins (Stxs) secreted by Shiga toxin-producing *E. coli* (STEC) [Lee M.S., Tesh V., 2019]. Humans contract STEC infections

by ingestion of contaminated food or water; every year STEC cause an estimated 2.8 million acute illnesses worldwide [Majowicz S.E., Scallan E. et al. 2014]. Shiga toxins can cause hemorrhagic colitis, which may progress to hemolytic-uremic syndrome (HUS), a severe and often fatal complication [Cody E.M., Dixon B.P., 2019; Bruyand M., Mariani-Kurkdjian P. et al. 2018].

Several studies showed that elimination of N-glycans from GTs may affect their activity [Mikolajczyk K., Kaczmarek R. et al. 2020]. The protein sequence of human Gb3/CD77 synthase includes two potential N-glycosylation sites at N_{121} and N_{203} (UniProt Q9NPC4, https://www.uniprot.org/). We found before that both N-glycosylation sites in Gb3/CD77 synthase produced in insect cells are occupied; we also showed that enzymatic deglycosylation of insect cell-derived recombinant human Gb3/CD77 synthase causes a complete loss of activity [Szymczak K., Kaczmarek R. et al. 2016]. In this study, using site-directed mutagenesis, we generated six N-glycosylation variants of the human Gb3/CD77 synthase (three for Gb3/CD77 synthase and three for the mutein) with substituted N-glycosylation sequons, and analyzed their activity in CHO-Lec2 cells transfected with vectors encoding the glycovariants. In order to elucidate the molecular backgrounds of altered Gb3/CD77 synthase activity, we evaluated expression levels of genes encoding the glycovariants, their subcellular localization in CHO-Lec2 and a potential influence of N-glycosylation on the enzyme secretion. Finally, we investigated whether CHO-Lec2 cells expressing the glycovariants revealed different sensitivity to Shiga toxins.

Results

Gb3/CD77 synthase contains two occupied N-glycosylation sites

Human Gb3/CD77 synthase contains two potential N-glycosylation sites: N_{121}-A-S and N_{203}-L-T (UniProt Q9NPC4, https://www.uniprot.org/) (Fig. 1). Previously, we showed that treatment of the enzyme with PNGase F abolished its *in vitro* activity [Szymczak K., Kaczmarek R. et al. 2016]. Six glycovariants were generated: four single mutants with p.S123A substitution (Q_{S123A} and E_{S123A} for Gb3/CD77 synthase and its mutein, respectively) and p.T205A substitution (Q_{T205A} and E_{T205A} for Gb3/CD77 synthase and its mutein, respectively), as well as two double mutants (Q_{S123A}/Q_{T205A} and E_{S123A}/E_{T205A}) (Fig. 1). The enzymes without any substitutions at N-glycosylation sites (fully N-glycosylated) are referred to as "Q_{full}" for the Gb3/CD77 synthase and "E_{full}" for the mutein.

In order to check whether the targeted sequons are N-glycosylated, CHO-Lec2 cells expressing the glycovariants were lysed and analyzed by western blotting. The human Gb3/CD77 synthase was detected using the monoclonal mouse anti-A4GALT antibody (clone 5C7). The occupancy of N-glycosylation sites was examined by comparing the electrophoretic mobility of the glycovariants with the fully N-glycosylated enzyme forms (Q_{full} and E_{full}). The mobility of single mutants Q_{S123A}, E_{S123A}, Q_{T205A} and E_{T205A} was almost the same, and their apparent molecular weight (MW) was lower (about 37 kDa) than their fully N-glycosylated Q_{full} and E_{full} counterparts (39 kDa) (Fig. 2A and Fig. 2B). The double-mutant glycovariants Q_{S123A}/Q_{T205A} and E_{S123A}/E_{T205A} revealed the lowest apparent MW (32 kDa) of all evaluated proteins, suggesting that both N-glycosylation sites of human Gb3/CD77 synthase are occupied (Fig. 2A and Fig. 2B).

To corroborate these results, CHO-Lec2 cells transfected with vectors encoding the glycovariants and fully N-glycosylated enzymes were lysed and treated with peptide-N-glycosidase F (PNGase F), which removes N-glycans from proteins, generated products whose electrophoretic mobility corresponded with the glycanless glycovariants Q_{S123A}/Q_{T205A} and E_{S123A}/E_{T205A} (Fig 2D and Fig. 2E). Moreover, CHO-Lec2 cells expressing the fully N-glycosylated enzymes (Q_{full} and E_{full}) were grown in the presence of tunicamycin, which completely inhibits N-glycosylation [Esko J.D., Bertozzi C. et al. 2017]. Both proteins showed similar apparent MW as glycovariants Q_{S123A}/Q_{T205A} and E_{S123A}/E_{T205A}, showing that elimination of N-glycans from these two sites strips the enzyme of all glycans (Fig. 2E and Fig. 2F). In summary, our results indicate that both N-glycosylation sites of human Gb3/CD77 synthase are occupied by N-glycans.

E_{S123A} and E_{T205A} glycovariants have opposing effects on Gb3/CD77 activity

To examine the activity of human Gb3/CD77 synthase glycovariants in CHO-Lec2 cells, presence of P1PK antigens (Gb3 and P1 for Gb3/CD77 synthase; Gb3, P1 and NOR for its mutein) was evaluated using flow cytometry (Fig. S1). Two anti-P1 antibodies were used: (1) anti-P1 (clone 650) that reacts with Gb3 and P1 and (2) anti-P1 (clone P3NIL100) that binds only to P1 (Table S1, Table S5). For detection of the NOR antigen, we used mouse monoclonal nor118 antibody (Table S5) [Duk M., Kusnierz-Alejska G. et al. 2005]. Quantitative analyses of Gb3, P1 and NOR antigens (determined by estimating antibody binding capacities) on CHO-Lec2 cells transfected with vectors encoding glycovariants showed various quantitative patterns, which are presented in Table 1A. The highest antibody

binding capacities (ABCs) of anti-P1 (650) antibody were found for Q_{S123A} and E_{full} clones, while anti-P1 (P3NIL100) showed highest ABC for Q_{full} and E_{full}. The lowest ABC values of anti-P1 (650 and P3NIL100) were found for double mutated glycovariants Q_{S123A}/Q_{T205A} and E_{S123A}/E_{T205A} (Fig. 3). These results suggest that the presence of N-glycan at N_{205} in human Gb3/CD77 synthase is essential for its activity. Surprisingly, the presence of N-glycan at N_{121} site seemed to hamper the activity of the enzyme.

To evaluate the activity of human Gb3/CD77 synthase *in vitro*, we used lysates prepared from CHO-Lec2 cells transfected with vectors encoding glycovariants in an enzyme assay using oligosaccharide-polyacrylamide (PAA) conjugates as acceptors. The amounts of reaction products were measured using anti-P1 (650 and P3NIL100) antibodies, anti-NOR antibody (nor118) and a color reaction monitored by A_{405nm}. Q_{full} and E_{full} showed the highest activity (Fig. S2A and Fig. S2B). Activities of the single-mutant glycovariants were reduced (except for Q_{S123A} with the P1 precursor nLc4-PAA, whose activity was the same as that of Q_{full}'s), while the double-mutant glycovariants Q_{S123A}/Q_{T205A} and E_{S123A}/E_{T205A} were inactive (Fig. S2A and Fig. S2B). These results suggested that a lack of either N-glycan (N_{121} or N_{203}) caused a decrease in the enzyme activity, while the enzymes completely devoid of N-glycans were inactive *in vitro*. All the activity data are summarized in Table 1A, Table 1B and Table 1C.

Since P1PK GSLs are the main products of human Gb3/CD77 synthase, we analyzed neutral glycosphingolipids isolated from CHO-Lec2 cells transfected with vectors encoding glycovariants with thin-layer chromatography (HPTLC, Fig. 4A and Fig. 4B). In orcinol staining, we found that Gb3Cer and Gb4Cer were the predominant GSLs in all samples. In addition, we showed that cells expressing E_{full} and E_{S123A} glycovariants produced larger amounts of NOR glycosphingolipids than cells expressing other mutein glycovariants (Fig 4B). Neither Q- nor E-derived glycovariants produced GSLs detectable with anti-P1 (P3NIL100) antibody (Fig. 4A and Fig. 4B), which suggests that human Gb3/CD77 synthase is unable to synthesize the P1 antigen in CHO-Lec2 cells, most probably due to lack of the acceptor (paragloboside).

The identities of glycosphingolipids derived from transfected cells were confirmed using MALDI-TOF mass spectrometry (Fig. S3 and Fig. S4). The reflectron-positive mode spectrum showed several clusters of monosodiated adduct ions $[M+Na]^+$ corresponding to glucosylceramide (GlcCer), lactosylceramide (LacCer) and certain globo-series GSLs (e.g. Gb3, NOR1). The mass differences between the ions (mostly ~ 28 Da, which is the molecular

mass of two methylene groups) corresponded to isoforms with ceramides having acyl groups of different lengths (e.g. 16:0, 18:0, 20:0, 22:0) but the same long-chain base (d18:1 sphingosine). No P1 antigen-corresponding structures were identified (Fig. S3 and Fig. S4).

Since levels of the P1PK antigens may correlate with the levels of *A4GALT* transcripts in the cells, we examined the expression of genes encoding glycovariants of Q and E enzymes in CHO-Lec2 cells using qPCR. The levels of all transcripts were upregulated in the transfected cells in comparison to the non-transfected CHO-Lec2 cells (Fig. S5). The mean threshold cycle (C_T) revealed no significant differences in transcript levels between cells transfected with different glycovariants (Fig. S5).

There is a general agreement that GSLs are the main acceptors for human Gb3/CD77 synthase, although it was shown recently that the enzyme can also use glycoproteins [Szymczak-Kulus K., Weidler S. et al. 2019; Stenfelt L., Westman J.S. et al 2019]. To find out if the glycovariants differ in acceptor preferences, we analyzed the presence of P1 glycotope on glycoproteins derived from CHO-Lec2 cells transfected with vectors encoding different glycovariants. Using western blotting and anti-P1 antibodies, we found that lysates of cells expressing the Q_{full} and E_{S123A} enzymes revealed the strongest binding (Fig. S6A and Fig. S6B, respectively), with the E_{S123A} reaction being markedly stronger than its fully glycosylated counterpart (E_{full}). Lysates from the Q_{T205A}- and E_{T205A}-expressing cells produced weakly recognized glycoproteins, with a slightly stronger reaction in the case of E enzyme (Fig. S6A and Fig. S6B). No binding of anti-P1 (650) antibody was detected in the case of double-mutant glycovariants Q_{S123A}/Q_{T205A} and E_{S123A}/E_{T205A}, although anti-P1 (P3NIL100) weakly recognized a few bands (Fig. S6A and Fig. S6B). These data may suggest that the fully N-glycosylated human Gb3/CD77 synthase and the majority of its glycovariants can efficiently use glycoproteins as acceptors. Moreover, the E_{S123A} enzyme seems to have a higher affinity to glycoprotein acceptors than the other glycovariants.

Cells expressing Gb3/CD77 synthase glycovariants show increased sensitivities to Shiga toxins

Since the main receptor for Shiga toxins 1 and 2 is Gb3, we evaluated the sensitivity of CHO-Lec2 cells transfected with vectors encoding glycovariants of human Gb3/CD77 synthase to these toxins. We found that sensitivity of the cells expressing single-mutant glycovariants of Q and E treated with Stx1 and Stx2 holotoxins was almost the same as that of the cells expressing fully N-glycosylated enzymes (Fig. 5A and Fig. 5B). To our surprise, the

CHO-Lec2 cells expressing double-mutant glycovariants (Q_{S123A}/Q_{T205A} and E_{S123A}/E_{T205A}) were still more sensitive to both Stxs than non-transfected CHO-Lec2 cells, which do not express receptors for Shiga toxins. Viability of Q_{S123A}/Q_{T205A} cells was 34% and 35% for Stx1 and 2, respectively (Fig. 5A); viability of E_{S123A}/E_{T205A} cells was 37% for Stx1 and 39% for Stx2 (Fig. 5B). Cells expressing the single-mutant Q glycovariants and Q_{full} were 34-42% and 25-44% viable after treatment with Stx1 and Stx2, respectively; viability of cells expressing E_{full} and the single-mutant E glycovariants was 23-24% and 22-24% upon exposure to Stx1 and Stx2, respectively (Fig. 5A and Fig. 5B). Viability correlated with Gb3 expression levels on the cells expressing single-mutant glycovariants, while the cells expressing double-mutant glycovariants likely produced trace amounts of Gb3 which sufficed to mediate cytotoxicity of Shiga toxins.

The N_{203} glycan in Gb3/CD77 synthase determines its subcellular localization

To determine whether N-glycosylation affects trafficking and localization of human Gb3/CD77 synthase, we evaluated the CHO-Lec2 cells transfected with vectors encoding glycovariants using 5C7 monoclonal antibody in immunofluorescence microscopy. It is generally assumed that the human Gb3/CD77 synthase, similarly to other GTs belonging to the glycosyltransferase family 32, is a Golgi-resident enzyme (www.cazy.org). Co-immunostaining of Q_{full}, E_{full}, Q_{S123A}, E_{S123A}, Q_{T205A} and E_{T205A} glycovariants with anti-A4GALT antibody and anti-syntaxin16 as a marker of the *trans*-Golgi cisternae revealed that all these enzymes localized in *trans*-Golgi (Fig. 6 and Fig. 7). Q_{T205A}, E_{T205A}, Q_{S123A}/Q_{T205A} and E_{S123A}/E_{T205A} glycovariants co-localized with anti-calnexin antibody, which recognizes ER-resident proteins (Fig. 6 and Fig. 7). Moreover, the glycovariants Q_{T205A} and E_{T205A} co-localized with both syntaxin 16 and calnexin, revealing that these enzymes localized both in the *trans*-Golgi and the ER. In contrast, the double-mutant glycovariants Q_{S123A}/Q_{T205A} and E_{S123A}/E_{T205A} accumulated in the ER only (Fig. 6 and Fig. 7). The residual signals derived from anti-LAMP1 (marker of lysosomes) and anti-A4GALT antibodies were found only in the case of Q_{S123A}/Q_{T205A} glycovariant (Fig. 6). Thus, it may be concluded that the fully N-glycosylated enzymes (Q_{full} and E_{full}), as well as Q_{S123A} and E_{S123A} glycovariants exit the ER properly and localize in the Golgi. In contrast, the glycovariants with substituted N_{203} site (Q_{T205A} and E_{T205A}) partially fail to leave the ER. The glycanless variants (Q_{S123A}/Q_{T205A} and E_{S123A}/E_{T205A}) were found only in the ER. These results show that N-glycan at position N_{203}

plays a crucial role in trafficking and proper subcellular localization of the human Gb3/CD77 synthase.

All glycovariants of human Gb3/CD77 synthase were further evaluated using immunogold reaction with 5C7 monoclonal antibody (diluted 1:10). We found that the glycovariants localized in the ER and/or Golgi (Fig. S7 and Fig. S8). In addition, we observed increased number of gold nanoparticles corresponding to fully N-glycosylated Q_{full} and E_{full} enzymes as well as Q_{S123A} and E_{S123A} glycovariants, when comparing to glycovariants with p.T205A substitution (Fig. S7 and Fig. S8). In contrast, the double-mutant Q_{S123A}/Q_{T205A} and E_{S123A}/E_{T205A} glycovariants showed decreased numbers of gold nanoparticles in comparison to other glycovariants (Fig. S7 and Fig. S8). These data suggest that disruption of the N_{121} site did not influenced enzyme synthesis in the cells, in contrast to the glycovariants without N-glycan at N_{203} site which seemed to be synthesized less efficiently.

Some of Gb3/CD77 synthase glycovariants are efficiently secreted

It was shown previously that recombinant glycosyltransferases may be secreted to the medium, despite the lack of any secretion signal sequence, i.e. human β1,4-galactosyltransferase 4 overexpressed in the HEK293T cells [Lopez LC, Youakim A, 1991, Shauchuk A, Szulc B, 2020]. Using western blotting and 5C7 monoclonal antibody, we found that CHO-Lec2 cells transfected with vectors encoding some of the studied glycovariants efficiently secreted those enzymes to the medium. The E_{S123A} glycovariant and, to a lesser extent, Q_{S123A} were secreted best, while the presence of Q_{full} and E_{full} was markedly reduced in the medium (Fig. S9). Other glycovariants were not detected at all, suggesting that the N_{121} site plays a crucial role in secretion of Gb3/CD77 synthase (Fig. S9).

Discussion

N-glycosylation of proteins has important and well-defined functions, but one somewhat overlooked function is regulation of glycosyltransferase activity. The available data on that role were recently reviewed in [Mikolajczyk K., Kaczmarek R. et al. 2020]. Elimination of N-glycans usually does not directly impact catalytic functions, but it may affect the enzyme stability, subcellular localization, secretion and ability to oligomerize, which may influence the enzyme activity. In most cases, altered activity of a non-glycosylated or underglycosylated enzyme is caused by misfolding and accumulation in the ER, which

prevents transport to the proper cellular compartment and/or its degradation caused by enhanced aggregation [Mikolajczyk K., Kaczmarek R. et al. 2020; Skropeta D., 2009].

Contrary to the old rule “one enzyme - one linkage” some GTs are promiscuous [Biswas A., Thattai M., 2020]. One example is human Gb3/CD77 synthase, which can recognize two different disaccharide acceptors, giving rise to Gb3 and the P1 antigen [Kaczmarek R., Mikolajewicz K. et al. 2016]. A single amino acid substitution p.Q211E, which enables attachment of galactose to another terminal monosaccharide, GalNAc, creating Galα1→4GalNAcβ structure, makes the enzyme even more promiscuous. Extension of acceptor specificity via a single amino acid substitution is a rare phenomenon compared to the more common donor specificity changes. For example, the donor specificity of the ABO transferase depends on two amino acids: the enzyme with c.796C>A (p.L266M) and c.803G>C (p.G268A) substitutions attaches galactose instead of *N*-acetylgalactosamine to the acceptor. Moreover, the cisAB enzyme (with p.L266G substitution) can use either donor substrate, producing both the A and B antigens [Wagner G.K., Pesnot T. et al 2015; Ramakrishnan B., Qasba P.K. et al. 2002].

To date, no studies have fully investigated the influence of N-glycosylation on human Gb3/CD77 synthase activity. Previously, we showed that deglycosylated recombinant catalytic domain of Gb3/CD77 synthase expressed in insect cells is inactive [Szymczak K., Kaczmarek R. et al. 2016]. In this study, we tried to answer the question whether these N-glycosylation sites are occupied by N-glycans, and how each of these N-glycans or their lack affects the enzyme activity. To that end, we used the site-directed mutagenesis to replace the third amino acid at one or both of the two canonical N-glycosylation sequons with alanine to generate constructs encoding glycovariants [Kaczmarek R., Mikolajewicz K. et al. 2016; Czerwinski M., Kern J. et al. 2007; Leong S.R., Kabakoff R.C. et al. 1994]. That result prompted us to comprehensively evaluate the influence of N-glycosylation on the Gb3/CD77 synthase activity using full-length enzyme expressed in CHO-Lec-2 cells, which were selected because they do not express an endogenous Gb3/CD77 synthase and are deficient in CMP-sialic acid transporter [Stanley P. 1983; Patnaik S.K., Stanley P. 2006]. Thus, they are incapable of sialylation, leaving a large proportion of acceptors available for α-galactosylation, which otherwise could be consumed by sialyltransferases.

Human Gb3/CD77 synthase contains two N-glycosylation sites (N_{121} and N_{203}). We found that elimination of N-glycans from the enzyme markedly affects its enzymatic activity and that disruption of each N-glycosylation site produces strikingly different effects. In flow

cytometry, the Q_{S123A} glycovariant, which lacks the N-glycan at N_{121}, had increased activity in comparison to the fully N-glycosylated enzyme. Interestingly, the same glycovariant had similar activity to the Q_{full}, when analyzed *in vitro* (using PAA-conjugates). In contrast, the E_{S123A} glycovariant exhibited approximately the same activity as the E_{full} enzyme both in flow cytometry and *in vitro*. In microscopy, both glycovariants with substituted N_{121} site localized in the Golgi, similarly to the fully N-glycosylated enzyme. These findings suggest that the N-glycan linked to N_{121} suppresses the enzyme activity. In the case of Q_{S123A} glycovariant, the immunogold reaction results indicate that its hyperactivity activity is related to increased synthesis of the enzyme. The elevated amount of Q_{S123A} enzyme in cells, together with proper intracellular localization, may increase the production of P1PK antigens in comparison to the wild-type enzyme. In addition, the N-glycan at position N_{121} seemed to affect the secretion of the enzyme from CHO-Lec2 cells to the medium. In summary, we postulate that the N-glycan linked to N_{121} affects the enzyme activity and secretion.

In contrast, we found that the presence of N-glycan at position N_{203} in Gb3/CD77 synthase plays a different role, being critical for the enzyme activity. Flow cytometry and *in vitro* assays revealed markedly reduced quantities of Gb3 and P1 antigen produced by CHO-Lec2 cells expressing the Q_{T205A} and E_{T205A} glycovariants in comparison to the E_{full} enzyme. Immunofluorescence analysis showed that both Q_{T205A} and E_{T205A} localized in two distinct compartments of the cell: in the ER and the *trans*-Golgi. The ER portions of the enzymes were likely inactive. Thus, partial mislocalization in the ER may affect the overall measurable enzyme activity because only the Golgi-resident enzyme is capable to perform its catalytic functions. Moreover, the decreased enzyme activity of the glycoforms missing the N_{203} glycan may be associated with reduced enzyme solubility because the Q_{T205A} and E_{T205A} glycovariants were not detected in culture media, suggesting their poor secretion. These results suggest that the N-glycan at position N_{203} site plays a crucial role in subcellular localization, trafficking and secretion of the enzyme, thus affecting the specific enzyme activity.

The double-mutant glycovariants Q_{S123A}/Q_{T205A} and E_{S123A}/E_{T205A} of human Gb3/CD77 synthase showed only residual activity. In our opinion, the loss of activity is caused by altered subcellular localization because both enzymes were found only in the ER. Also, we did not detect any enzymatic activity of these glycovariants in cell lysates, which may have been caused by a decrease in solubility. These glycovariants were not detectable in the culture medium either. Overall, these results show that N-glycosylation of human

Gb3/CD77 synthase, especially at position N_{203}, is essential for trafficking, proper subcellular localization and activity, but the two N-glycans play vastly different roles.

An increase in the activity of a glycosyltransferase upon eliminating its N-glycans is a rare phenomenon. Our data suggest that human Gb3/CD77 synthase with substituted N_{121} site exhibits elevated activity in comparison to the wild-type enzyme. One limitation of site-directed mutagenesis in studies of glycosylation is that it inherently changes the protein backbone, the potential impact of which cannot be disregarded when interpreting the effects of mutating N-glycosylation sites. Notably, human α2,3-sialyltransferase-II ST3Gal-II contains two N-glycosylation sites at N_{92} and N_{211} and shows increased activity with a disrupted N_{92} site, even though it is not occupied by N-glycan in the wild-type enzyme [Ruggiero F.M., Vilcaes A.A. et al. 2015]. We cannot rule out that the effects of disrupting N_{121} in Gb3/CD77 synthase have a similar molecular background. However, the N_{121} sequon is occupied by an N-glycan and no gain-of-function mutations are known for Gb3/CD77 synthase other than c.631C>G (underlying the p.Q211E substitution). The other known missense mutations in *A4GALT* are either neutral or cause a loss of activity, which suggests that the gain of function observed upon disruption of N_{121} is brought about by the loss of N-glycan.

Several studies showed that removal of N-glycans from GTs may cause a decrease in activity (human α1,3/4-fucosyltransferase-III [Christensen L.L., Jensen U.B. et al. 2000]) and/or its complete loss (murine β1,3-galactosyltransferase-IV B3Gal-T4 [Martina J.A., Daniotti J.L. et al. 2000]). The molecular background of activity change may be related to (1) enzyme misfolding, like for murine ST3Gal-V [Uemura S., Kurose T. et al. 2006], (2) altered subcellular localization of the enzyme, e.g. chicken α2,8-sialyltransferase-I [Martina J.A., Daniotti J.L. et al. 1998], (3) changed kinetic parameters, such as rat β1,4-*N*-acetylglucosaminyltransferase-III [Nagai K., Ihara Y. et al 1997], (4) a decrease in the enzyme solubility, such as human β1,3-*N*-acetylglucosaminyltransferase-II [Kato T., Suzuki M. et al. 2005], (5) enzyme aggregation, such as human α2,3-sialyltransferase-I ST3Gal-I [Jeanneau C., Chazalet V. et al. 2004]. Generally, it may be assumed that enzymes that fail to exit the ER are degraded, so they cannot reveal any activity, as was shown for plant β1,2-xylotransferase from *Arabidopsis thaliana* [Pagny S., Bouissonnie F. et al. 2003]. It should be noted, however, that usually none of these mechanisms contributes to the decrease in enzyme activity independently. In glycoproteins carrying multiple N-glycans, individual chains may vary in importance. In the case of human Gb3/CD77 synthase, its two N-glycans seem to have

opposing effects: increasing the activity in the case of N_{121}, and decreasing the activity in the case of N_{203}. While N-glycan at N_{203} is probably necessary for folding and/or solubility of the enzyme, the role of N_{121} is less clear. We hypothesize that N-glycan at N_{121} in the Q enzyme hampers catalytic functions (for example, due to steric hindrance at the active site). Interestingly, the E enzyme does not show an increase in activity upon eliminating the same N-glycan, but the E mutein is already hyperactive and perhaps the p.Q211E substitution produces its maximum possible activity. Moreover, presence of N-glycans impact protein folding and oligomerization, so eliminating N-glycans may change GT activity by altering its ability to oligomerize. Oligomerization may influence subcellular localization in the ER and/or Golgi, and so indirectly the activity of a GT [Harrus D., Khoder-Agha F. et al. 2018; Nilsson T., Hoe M.H. et al. 1994]. Previously, we showed that the Q enzyme of human Gb3/CD77 synthase more readily forms homodimers than the E mutein [Kaczmarek R., Suchanowska A. et al. 2013]. It is possible that eliminating N-glycans affects the enzyme's capability to oligomerize, resulting in changes in activity.

Since Galα1→4Galβ structures are recognized by Shiga toxins, we examined the activities of glycovariants with glycoprotein acceptors as well as the sensitivity of CHO-Lec2 cells expressing these glycovariants to Shiga toxins. Strikingly, we found that all kinds of the glycovariants were able to synthesize enough receptors to mediate cytotoxic activity of Shiga toxins, even the double-mutant enzymes, which otherwise revealed only residual activity. Thus, it may be speculated that even small amounts of Gb3 produced by double-mutant glycovariants are sufficient to trigger the cytotoxic effects.

In summary, our study shows that human Gb3/CD77 synthase is N-glycosylated on both N-glycosylation sites (N_{121} and N_{203}), and that N-glycans attached to the N_{121} and N_{203} sites affect activity of the enzyme in different ways. The N-glycan at position N_{121} appears to curtail the enzyme activity. Moreover, when N-glycan at N_{121} site is missing, the secretion of the enzyme is increased, which may be indirectly associated with its increased solubility, inducing enzyme synthesis in the cells. On the other hand, the N-glycan at position N_{203} seems to be necessary for correct localization in the Golgi. The glycanless (double-mutant) variants were stuck in the ER and could not be efficiently secreted.

The dual role of N-glycosylation in the activity of human Gb3/CD77 synthase is intriguing. Attachment of glycans facilitates and is often necessary for the folding of nascent proteins, so a loss of function is an expected corollary of disrupted glycosylation. Consequently, a gain of function associated with underglycosylation is counterintuitive. In the

case of Gb3/CD77 synthase, the unexpected role of N_{121}-linked glycan may have several interesting implications. It may represent a novel regulatory mechanism of preventing potentially detrimental effects of hyperactivity. Hyperactive enzymes may cause serious disorders. One example is the human serine protease coagulation factor IX (FIX), whose hyperfunctional variants are ~5-8-fold more active than the normal FIX and cause hereditary thrombophilias [Simioni P., Tormene D. et al. 2009; Wu W., Xiao L. et al. 2021]. Alternatively, the N_{121}-linked glycan may toggle substrate preferences of Gb3/CD77 synthase between glycosphingolipids and glycoproteins. Notably, avian Gb3/CD77 synthases readily use glycoproteins as acceptors, in contrast to the human enzymes, which use mainly glycosphingolipids [Bereznicka A., Modlinska A. et al. 2019]. N-glycosylation of avian Gb3/CD77 synthases has not been studied and perhaps is the missing link in our understanding of this major interspecies difference. In either scenario, mechanistic aspects of the unusual role of N_{121} glycan will require further studies.

Materials and methods

Antibodies

Mouse monoclonal antibody (clone 5C7) was produced by immunization of C57Bl/6J mice with four subcutaneous injections of the purified human Gb3/CD77 synthase with p.Q211E substitution expressed in insect cells [Kaczmarek R., Duk M. et al. 2016] emulsified in incomplete Freund's adjuvant (Sigma-Aldrich, St. Louis, MO). Hybridoma secreting antibodies were produced by fusing immune splenocytes with Sp 2.0-Ag14 mouse myeloma using 50% PEG 1500 solution (Sigma-Aldrich, St. Louis, MO) and subcloned by limiting dilution according to standard methodology [Miazek A., Brockhaus M. et al.1997].

Site-directed mutagenesis

The *A4GALT* gene (NG_007495.2) encoding full-length Gb3/CD77 synthase was used for site-directed mutagenesis, as described previously [Kaczmarek R, Mikolajewicz K. et al. 2016]. Briefly, two N-glycosylation sequons N_{121}-A-S and N_{203}-L-T were disrupted by introducing a codon for alanine in place of serine or threonine, respectively. In the first PCR reaction, two fragments of *A4GALT* gene were created, each containing the overlapping site with an introduced mutation. In the second reaction, the PCR products were duplexed to generate new template DNA. During the overlap extension phase, each fused product was amplified using primers complementary to the pCAG vector (kindly provided by Dr. Peter W.

Andrews, University of Sheffield, Sheffield, UK) (PCAG For and PCAG Rev). The resulting full-length gene fragments were digested with XhoI and NotI (Fermentas, Vilnius, Lithuania), cloned into appropriately digested pCAG vector and sequenced (Genomed, Warsaw, Poland) using primers PkSeqFor and PkSeqRev (listed in Table S1). The plasmids were purified using maxi prep kit (Qiagen, Venlo, Netherlands) according to the manufacturer's instruction. The PCR reaction was performed in a MJ Mini gradient PCR thermal cycler (BioRad, Hercules, CA, USA). 20 µl reaction mixture contained: approximately 200 ng of the template DNA, 0.2 mM forward and reverse primers, 0.2 mM dNTPs, 1.5 mM $MgCl_2$, HF polymerase buffer (1:5 dilution), 1 unit Phusion High-Fidelity DNA Polymerase (Fermentas, Vilnius, Lithuania). The DNA fragments were purified with a gel extraction kit (Gel-Out, A&A Biotechnology, Gdynia, Poland). The sequences of primers are shown in Table S1, and the conditions of PCR reactions are shown in Table S2.

Cell culture and transfection

CHO-Lec2 cells were obtained from the American Type Culture Collection (Rockville, MD, USA). The cells were grown and maintained in a humidified incubator with 5% CO_2 at 37°C used DMEM F12 medium (Thermo Fischer Scientific, Inc., Waltham, MA, USA) with 10% fetal bovine serum (Gibco, Inc., Waltham, MA, USA) and Pen-Strep (Gibco, Inc., Waltham, MA, USA). Culture medium was changed every second or third day, and after reaching 85-90% confluence, the cells were subcultured by treatment with trypsin (0.25% trypsin, 137 mM NaCl, 4.3 mM $NaHCO_3$, 5.4 mM KCl, 5.6 mM glucose, 0.014 mM phenol red, 0.7 mM EDTA), harvested, centrifuged at 800 x g for 5 min, resuspended in fresh medium and seeded to new tissue culture plates. One day before transfection, cells were seeded at 2 x 10^5 cells per well in six-well plates, giving at day of transfection about 60% confluence. The medium was replaced with fresh DMEM F12 (without FBS), and after 4 h the cells were transfected using 60 µg polyethyleimine (PEI, Polysciences, Warrington, PA, USA). Plasmid DNA in an amount of 1.5 µg was diluted in buffer containing 0.15 M NaCl and 20 mM HEPES (pH 7.5) and then mixed with PEI. The transfection mixture was incubated for 20 min at room temperature and then added dropwise to each well. After 48h medium was replaced with fresh DMEM F12 with 10% FBS and gradient concentration (5, 10, 20 and 50 µg/ml) of puromycin (Sigma-Aldrich, St. Louis, MO). The medium with antibiotic was changed daily for 10 days and then every 2 days. Selection was carried out until the non-transfected control cells were dead, and then cells were sorted using FACS. The cells

were harvested using trypsin, washed and suspended in PBS containing 0.5% FBS and 5mM M EDTA at a density of 10^6 cells/ml. After 1 h incubation at 4°C with anti-P1 (650 and P3NIL100) antibody (1:200 or 1:400, respectively), the cells were washed with PBS containing 0.5% FBS and 1 h incubated with FITC-conjugated goat anti-murine or goat anti-human $F(ab')_2$ antibodies, respectively. Before cell sorting the cells were filtered through a tubes with cell strainer (Falcon® Round-Bottom Tubes with Cell Strainer Cap, Thermo Fisher Scientific, Waltham, MA, USA) to remove cell aggregates. The analysis was carried out using FACS Aria I cell sorter with FACSDiva software (Becton Dickinson).

Western blotting and secretion analysis

The proteins were separated in the presence of SDS (Sodium Dodecyl Sulfate, Roth, Karlsruhe, Germany) using 10% polyacrylamide gel, according to the Laemmli method [Laemmli U.K., 1970] and visualized with CBB (Coomassie Brilliant Blue R-250, Roth, Karlsruhe, Germany) or transferred to nitrocellulose membrane (Sigma-Aldrich, St. Louis, MO). The PageRuler Prestained Protein Ladder (Thermo Fisher Scientific, Waltham, MA, USA) was used as a protein standard. The proteins fractionated by SDS-PAGE were transferred to the nitrocellulose membrane (Roth) according to the method of Towbin et al. [Towbin H., Staehelin T. et al. 1979] and detected with mouse anti-A4GALT monoclonal antibody (hybridoma supernatant diluted 1:10, 5C7 clone). For secretion analysis we used the supernatant collected from about 95% confluent cell cultures.

PNGase F digestion

Digestion of CHO-Lec2 protein lysates by PNGase F was performed as described [Maszczak-Seneczko D., Olczak T. et al. 2011] in denaturing conditions. Briefly, 1 µl of 10% SDS and 0.7 µl 1M DTT was added to 50 µg of transfected or untransfected CHO-Lec2 cell lysates and the samples were incubated in 95˚C for 5 minutes. The deglycosylation reaction was carried out with 500 units of PNGase F for 3 h at 37°C in a final volume of 20 µl. The reaction was stopped with SDS sample buffer and the products were analyzed by immunoblotting. PNGase F digestion in native conditions was carried out without denaturing reagents and skipped incubation at 95°C. Then, the products were used for enzyme activity examination with oligosaccharide-polyacrylamide (PAA) conjugates [Kaczmarek R., Duk M. et al. 2016].

Enzyme activity in cell lysates

CHO-Lec2 cells transfected with vectors encoding Gb3/CD77 synthase with substituted N-glycosylation sites were harvested and lysed according to [Cheng C., Guo J.Y. et al. 2016]. The buffer exchange (from Tris-HCl pH 7.4 to 50 mM sodium cacodylate pH 7.3) was carried out using Amicon Pro 10 kDa cut-off membranes. The enzymatic activity was evaluated by ELISA with oligosaccharide-polyacrylamide (PAA) conjugates [Kaczmarek R., Duk M. et al. 2016]. UDP-Gal (Sigma-Aldrich, St. Louis, MO) was used as a donor and three different conjugates were used as acceptors: Galß1,4Glc-PAA (Lac-PAA, the precursor of Gb3), Galß1,4GlcNAcß1,3Galß1,4Glc-PAA (nLc4-PAA, the precursor of P1), GalNAcß1,3Galα1,4Galß1,4Glc-PAA (Gb4-PAA, the precursor of NOR1) [Tuzikov A., Chinarev A. et al. 2021; Bovin N.V., 1998]. ELISA microtiter plates (Nunc, MaxiSorp, Roeskilde, Denmark) were coated overnight in 4°C with conjugates (2 µg/well) in phosphorane buffer (50 mM, pH 7.4). Enzyme samples (100 µg/well) in cacodylate buffer containing Mn^{2+} and the donor substrate (50 mM sodium cacodylate pH 7.4, 14 mM $MnCl_2$, 200 µM UDP-Gal, pH 6.32) were loaded in triplicates. The reactions were run overnight (16-18 h) in 37°C. The plates were then washed twice with distilled water and thrice with PBST (137 mM NaCl, 2.7 mM KCl, 10 mM Na_2HPO_4, 1.8 mM KH_2PO_4, 0.05% Tween 20) and blocked with 5% BSA in PBS-T. Next, dilutions of antibodies recognizing the reaction products (1:50, 1:100 and 1:100 for anti-P1 P3NIL100, anti-P1 650 and anti-NOR nor188, respectively) were added and incubated for 90 minutes in room temperature, followed by sequential 1-hour incubation with biotinylated anti-mouse or anti-human IgM antibody (each diluted 1:1000) and ExtrAvidin-alkaline phosphatase conjugate (diluted 1:10000). Wash steps were carried out using PBS-T/1% BSA. Finally, color reactions were developed with *p*-nitrophenyl phosphate (1 mg/ml in Tris-HCl with 1 mM $MgCl_2$) (Sigma-Aldrich, St. Louis, MO). Plates were read using 2300 EnSpire Multilabel Reader (PerkinElmer, Waltham, MA) at 405 nm at several time points within 1 hour. Data were analyzed using Microsoft Office Excel (Microsoft Corp, Redmond, WA). Negative controls were set up by adding incomplete reaction mixtures (lacking UDP-Gal or enzyme) to coated wells; by adding complete reaction mixtures to uncoated wells; or by omitting primary or secondary antibodies.

Flow cytometry

The cells were incubated with 100 µl appropriately diluted primary antibodies (anti-P1 P3NIL100 1:200, anti-P1 650 1:400, anti-NOR nor118 1:20) for 60 min on ice. Then the cells were washed (all washes and dilutions were done with PBS) and incubated with 100 µl

(diluted 1:50) FITC-labeled anti-mouse IgM antibody for 40 min on ice in the dark. The cells were washed and approximately 5 x 10^5 cells were suspended in 750 µl of cold PBS and analyzed by flow cytometry using FACSCalibur (BD Biosciences, Franklin Lakes, NJ, USA). The number of events analyzed was 10000 / gated cell population. The analysis of the results was carried out using Flowing software (Perttu Terho, University of Turku, Turku, Finland) [Sahraneshin Samani F., Moore J.K. et al. 2014]. For quantification of cell surface antigens we used Quantum beads (Bio-Rad, Hercules, CA,USA) which carry defined quantities of FITC, and thus allow plotting calibration curves (mean fluorescence intensity versus Molecules of Equivalent Soluble Fluorochrome units). The cells were then analyzed by flow cytometry and the antibody binding capacity (ABC, the number of antibody molecules bound per cell) was calculated by interpolation from the calibration curve as described in the manufacturer's protocol and based on the fluorophore-to-protein molar ratios of the FITC-antibody conjugates. Negative control results (secondary antibody only) were subtracted from the sample results to obtain specific antibody binding capacities.

Extraction and purification of glycosphingolipids from CHO-Lec2

The isolation and fractionation of glycosphingolipids and the orcinol staining were performed as described previously [Duk M., Reinhold B.B. et al. 2001]. Cellular lipids were extracted with chloroform/methanol from 10^7 transfected or non-transfected CHO-Lec2 cells. The neutral glycosphingolipids were separated from the phospholipids and gangliosides, purified in peracetylated form, de-O-acetylated, and desalted. Glycosphingolipid samples were solubilized in chloroform/methanol (2:1, v/v), applied to HPTLC plates (Kieselgel 60, Merck, Darmstadt, Germany), and developed with chloroform/methanol/water (55:45:9, v/v/v). The dried plates were immersed in 0.05 % polyisobutylmethacrylate (Sigma-Aldrich, St. Louis, MO) in hexane for 1 min, dried, sprayed with TBS (0.05 M Tris buffer, 0.15 M NaCl (pH 7.4), and blocked in 5 % HSA. For antibody assays, the plates were successively overlaid with 1) primary antibody diluted in TBS/1 % BSA (TBS-BSA) for 1–1.5 h; 2) biotinylated goat anti-mouse Ig antibody (Dako, Glostrup, Denmark), diluted 1:5000 with TBS-BSA; 3) ExtrAvidin-alkaline phosphatase conjugate (Sigma-Aldrich, St. Louis, MO, USA) diluted 1:1000 with TBS/ BSA/0.2 % Tween20 for 1 h; and 4) the substrate solution (nitro blue tetrazolium/5-bromo-4-chloro-3-indolyl phosphate, Sigma-Aldrich, St. Louis, MO). Other details were as described previously [Duk M., Reinhold B.B. et al. 2001; Duk M., Singh S. et al. 2007]. Each HPTLC experiment was repeated three times.

HPTLC orcinol staining

Orcinol staining was performed using standard procedures as previously described [Kuśnierz-Alejska G., Duk M. et al. 1999; Duk M., Reinhold B.B. et al. 2001]. Briefly, dried HPTLC plates were sprayed with a solution of orcinol (0.2% w/v) in 3 M aqueous sulfuric acid and incubated in an oven at 110°C for 10 minutes.

Quantitative analysis of transcripts level

Total RNA from transfected or untransfected CHO-Lec2 cells was prepared using Universal RNA Purification Kit (Eurx, Gdansk, Poland) and the complementary DNAs (cDNAs) were synthesized using SuperScript III First-Strand Synthesis kit (Life Technologies, Carlsbad, CA, USA) with oligo(dT) primers. Quantitative polymerase chain reaction (qPCR) was performed on 30 ng of cDNA using the 7500 Fast Real-Time PCR System (Life Technologies, Carlsbad, CA, USA), according to the manufacturer's instruction. The *A4GALT* transcripts were detected with Custom TaqMan Gene Expression Assay. The ORF sequences were chosen in assay design to enable detection of transcripts originating from plasmids. A predesigned TaqMan assay targeting exon 2–3 boundary (Hs00213726_m1; Life Technologies) was also used to ensure equal amount of the endogenous *A4GALT* transcript in transfected and untransfected cells. The transcript quantities were normalized to hamster *GAPDH* endogenous control (sequence in Table S3B). All samples were run in triplicates. Data were analyzed using Sequence Detection software Version 1.3.1 (Life Technologies, Carlsbad, CA, USA). Target nucleotide sequences are shown in Table S3, while qPCR conditions are in Table S4.

MALDI-TOF Mass Spectrometry of CHO-Lec2 GSLs

MALDI-TOF mass spectrometry was carried out on a MALDI TOF/TOF ultrafleXtreme™ instrument (BrukerDaltonics, Bremen, Germany). Samples were dissolved in chloroform:methanol (2:1, v/v). Norharmane (9H-Pyrido[3,4-b]indole, Sigma-Aldrich, St. Louis, MO) was used as a matrix (10 mg/ml, chloroform:methanol, 2:1, v/v). Spectra were scanned in the range of m/z 700–1600 in the reflectron-positive mode. External calibration was applied using the Peptide Calibration Standard II (BrukerDaltonics, Bremen, Germany).

Cytotoxicity assay

2 x 10^4 CHO-Lec2 cells were seeded in 96-well plates (Wuxi NEST Biotechnology Co., Ltd, China) in complete DMEM/F12. After 24 h the medium was replaced by 100 µl/well of serum-free DMEM/F12 containing 0.1, 0.5 and 1 ng/ml of Stx1 or Stx2 holotoxins (all concentrations were run in triplicates). After 20 h of toxin treatment, 20 µl/well of MTS tetrazolium compound (CellTiter 96® AQueous One Solution Assay, Promega, Madison, WI) was added. Plates were incubated in humidified, 5% CO_2 atmosphere for 2.5 h, then absorbance at 490 nm was recorded on ELISA plate reader. Background absorbance registered at zero cells/well was subtracted from the data and the absorbance of wells incubated in medium without addition of Stx was taken as 100% of cell viability. Each experiment was performed at least three times.

Immunolocalization of Gb3/CD77 synthase

Immunogold

For ultrastructural analysis in transmission electron microscopy (TEM) 5 x 10^6 transfected or untransfected CHO Lec2 cells were fixed in cooled 4% formaldehyde solution (FA), diluted in PBS for 20 min at room temperature (RT) (Thermo Fisher Scientific, Waltham, MA, USA). After fixation, the cells were scraped and the cell suspensions were centrifuged 3 times at 2100 x g for 8 minutes followed by rinsing the samples with PBS and distilled water. After adding 1 drop of bovine thrombin (Biomed, Lublin, Poland) to 2 drops of fibrinogen (1mg/ml; Sigma-Aldrich, St. Louis, MO; Merck KGaA) the cells were entrapped within the fibrin clots. Next, the cell clots were post-fixed for 7 min in 0.25% (w/v) osmium tetroxide OsO_4 diluted in PBS (Serva Electrophoresis, Heidelberg, Germany). Subsequently, the samples were rinsed with PBS 3 times for 5 min.

The cell clots were dehydrated in the increasing concentration of ethanol, EtOH 50%, 70%, 96%, 99,8% (Stanlab, Lublin, Poland) for 10 min at RT. Afterwards, the samples were incubated for 3 h at RT in the mixture of EtOH and LR White resin (Polysciences, Inc., Warrington, PA, USA) in the following proportions: 2:1, 1:1 and 1:2, respectively. Finally, the samples were embedded in pure resin. Polymerization of the resin blocks was carried out at 55°C for 48 h.

LR White blocks were cut into semithin, 600-nm-thick sections with the Histo Diamond Knife (Diatome, Nidau, Switzerland). The semithin sections were stained with a dye solution (Serva, Alchem, Toruń, Poland) and closed with a Euparal mounting agent (Carl

Roth, Mannheim, Germany), followed by examination on a light microscope in order to remove excessive resin and select a group of no fewer than 30 cells for TEM documentation. Finally, ultrathin, 70-nm-thick sections were cut with the Ultra 45° Diamond Knife (Diatome), arranged with a loop, and collected onto the dull side of nickel grids (200 mesh, Ted Pella, Redding, Ca, USA). Resin-embedded materials were prepared using an ultramicrotome Power Tome XL (RMC, Tucson, USA).

All incubation steps were performed on top of drops of appropriate reagents at RT. First, the ultrathin sections were incubated in 0.02 M glycine (Biotechnology grade, BioShop Canada Inc., Burlington, Canada), dissolved in PBS (1 time for 10 min) to quench free aldehyde groups, followed by gentle rinsing with PBS. Then, the cells were permeabilized 2 times for 5 min with 0.1% Triton X-100 (Reagent grade, BioShop), followed by washing 3 times for 5 min with PBS. In order to block non-specific antigen-binding sites, the grids were transferred for 1h to 1% bovine serum albumin PBS solution (Albumin fraction V, Carl Roth) and rinsed with PBS for 5 min. For immunogold reaction, the grids were incubated with mouse anti-A4GALT monoclonal antibody (hybridoma supernatant diluted 1:10, clone 5C7) for 1 h, followed by washing the sections in PBS 3 times for 5 min. Subsequently, secondary antibody conjugated with colloidal gold nanoAbcam, Cambridge, UK, preadsorbed) in 1% BSA in PBS (dilution 1:10) was applied for 1h (dark chamber).

Next, the grids were rinsed with PBS and distilled water, 6 times for 5 min. Additionally, the specimens were post-fixed with 1% glutaraldehyde (Serva Electrophoresis, Heidelberg, Germany) diluted in PBS for 5 min, followed by rinsing with distilled water 3 times for 5 min. To improve contrast, the ultrathin sections were counterstained with uranyl acetate (10 min) and lead citrate trihydrate (5 min) (Serva), and then rinsed 3 times in distilled water. The sections were then examined using TEM JEM-1011 (Jeol, Tokyo, Japan) with the accelerating voltage of 80kV. Digital micrographs were collected using TEM imaging platform iTEM1233 equipped with a Morada Camera (Olympus, Münster, Germany) at magnifications ranging from 4 to 50K.

Immunofluorescence

Millicell EZ slides were used for culturing cells prior to staining. Cells were fixed on the second day of culture with 4% paraformaldehyde (PFA) in PBS added onto slides for 5 minutes. Afterwards, cells were washed 3 times for 5 minutes with PBS. To inhibit non-specific binding sites the slides were incubated 1 h with blocking solution (1% (w/v) BSA and

0.1% (w/v) saponin in PBS). After blocking, cells were incubated with primary antibodies (Table S5) for 3 h at 37°C. Washing (3 x 5 min) was carried out with the blocking solution. Subsequently, slides were incubated with secondary antibodies (Table S5) for 1 h at 37°C. Counterstain with 4′,6-diamidino-2-phenylindole (DAPI, Sigma-Aldrich, St. Louis, MO) for 10 min at room temperature was performed for nuclei visualization. Finally, slides were mounted onto glass coverslips using fluorescence mounting medium (Dako). Slides were examined with a LEICA SP8 confocal microscope and pictures were analyzed using ImageJ software (NIH).

Acknowledgements

We thank M.Sc. Michal Kulus (Wroclaw Medical University, Department of Ultrastructural Research, Wroclaw, Poland) for statistical analysis of cytotoxicity assay results, and Dr. Maria Duk (Hirszfeld Institute of Immunology and Experimental Therapy, Wroclaw, Poland) for valuable discussions.

Abbreviations

GSL, glycosphingolipid; Gb3, globotriaosylceramide; RBC, red blood cell; Stx, Shiga toxin; STEC, Shiga toxin-producing *Escherichia coli*; Stx1B, Shiga toxin 1 B subunit; Stx2B, Shiga toxin 2 B subunit; ER, endoplasmic reticulum; HUS, hemolytic uremic syndrome; PNGase F, peptide-N-glycosidase F; TLC, thin-layer chromatography; HPTLC, high performance thin layer chromatography; qPCR, quantitative polymerase chain reaction; MALDI-TOF, matrix-assisted laser desorption/ionization-time of flight.

Data availability statement

Raw MS data of GSLs analyzed in the paper are available at the GlycoPOST, Announced ID GPST000166 (https://glycopost.glycosmos.org/).

Funding and additional information

This work was funded by the Ministry of Science and Higher Education of Poland "Diamentowy Grant" 0097/DIA/2017/46.

References

Agthe M, Garbers Y, Grötzinger J, Garbers C. Two N-Linked Glycans Differentially Control Maturation, Trafficking and Proteolysis, but not Activity of the IL-11 Receptor. *Cell Physiol Biochem*. 2018;45:2071-2085.

Akiyama H, Ide M, Yamaji T, Mizutani Y, Niimi Y, Mutoh T, Kamiguchi H, Hirabayashi Y. Galabiosylceramide is present in human cerebrospinal fluid. *Biochem Biophys Res Commun*. 2021;536:73-79.

Albesa-Jové D, Giganti D, Jackson M, Alzari PM, Guerin ME. Structure-function relationships of membrane-associated GT-B glycosyltransferases. *Glycobiology*. 2014;24:108-24.

Bereznicka A, Modlinska A, Duk M, Kaczmarek R, Szymczak-Kulus K, Mikolajczyk K, Kapczynska K, Wittek P, Park EY, Piasecki T, Czerwinski M. Avian glycosphingolipid antigens as receptors for Shiga toxin. Conference: Glyco25, XXV International Symposium on Glycoconjugates, 25 - 31.08 At: Milan, Italy.

Biswas A, Thattai M. Promiscuity and specificity of eukaryotic glycosyltransferases. *Biochem Soc Trans*. 2020;48:891-900.

Bohl T, Bai L, Li H. Recent Progress in Structural Studies on the GT-C Superfamily of Protein Glycosyltransferases. *Subcell Biochem*. 2021; 96:259-271.

Bovin NV. Polyacrylamide-based glycoconjugates as tools in glycobiology. *Glycoconj J*. 1998; 15: 431-46.

Breton C, Fournel-Gigleux S, Palcic MM. Recent structures, evolution and mechanisms of glycosyltransferases. *Curr Opin Struct Biol*. 2012; 5:540-9.

Bruyand M, Mariani-Kurkdjian P, Gouali M, de Valk H, King LA, Le Hello S, Bonacorsi S, Loirat C. Hemolytic uremic syndrome due to Shiga toxin-producing Escherichia coli infection. *Med Mal Infect*. 2018;48:167-174.

Cheng C, Guo JY, Geng F, Wu X, Cheng X, Li Q, Guo D. Analysis of SCAP N-glycosylation and Trafficking in Human Cells. *J. Vis. Exp*. 2016; 117: e54709.

Christensen LL, Jensen UB, Bross P, Orntoft TF. The C-terminal N-glycosylation sites of the human alpha1,3/4-fucosyltransferase III, -V, and -VI (hFucTIII, -V, adn -VI) are necessary for the expression of full enzyme activity. *Glycobiology*. 2000;10:931-9.

Cody EM, Dixon BP. Hemolytic Uremic Syndrome. *Pediatr Clin North Am*. 2019;66:235-246.

Cooling L. Blood Groups in Infection and Host Susceptibility. *Clin Microbiol Rev*. 2015;28:801-70.

Czerwinski M, Kern J, Grodecka M, Paprocka M, Krop-Watorek A, Wasniowska K. Mutational analysis of the N-glycosylation sites of Duffy antigen/receptor for chemokines. *Biochem Biophys Res Commun*. 2007;356:816-21.

Duk M, Kusnierz-Alejska G, Korchagina EY, Bovin NV, Bochenek S, Lisowska E. Anti-alpha-galactosyl antibodies recognizing epitopes terminating with alpha1,4-linked galactose: human natural and mouse monoclonal anti-NOR and anti-P1 antibodies. *Glycobiology*. 2005;15:109-18.

Duk M, Reinhold BB, Reinhold VN, Kusnierz-Alejska G, Lisowska E. Structure of a neutral glycosphingolipid recognized by human antibodies in polyagglutinable erythrocytes from the rare NOR phenotype. *J Biol Chem*. 2001;276:40574-82.

Duk M, Singh S, Reinhold VN, Krotkiewski H, Kurowska E, Lisowska E. Structures of unique globoside elongation products present in erythrocytes with a rare NOR phenotype. *Glycobiology*. 2007;17:304-12.

Esko JD, Bertozzi C, Schnaar. RL. 2017. Chemical Tools for Inhibiting Glycosylation. In Varki A, Cummings RD, Esko JD, Stanley P, Hart GW, Aebi M, Darvill AG, Kinoshita T, Packer NH, Prestegard JH, Schnaar RL, Seeberger PH, editors Essentials of Glycobiology. 3rd edition. Cold Spring Harbor (NY): Cold Spring Harbor Laboratory Press; 2015-2017.

Fiedler K, Simons K. The role of N-glycans in the secretory pathway. *Cell*. 1995;81:309-12.

Furukawa K, Kondo Y, Furukawa K. 2014. UDP-G al:Lactosylceramide Alpha 1,4-Galactosyltransferase (A4GALT). In: Taniguchi N., Honke K., Fukuda M., Narimatsu H.,Yamaguchi Y, Angata T. Handbook of Glycosyltransferases and Related Genes, pp. 141–147. Springer Japan, Tokyo.

Gavel Y, von Heijne G. Sequence differences between glycosylated and non-glycosylated Asn-X-Thr/Ser acceptor sites: implications for protein engineering. *Protein Eng*. 1990; 3: 433-42.

Geyer PE, Maak M, Nitsche U, Perl M, Novotny A, Slotta-Huspenina J, Dransart E, Holtorf A, Johannes L, Janssen KP. Gastric Adenocarcinomas Express the Glycosphingolipid Gb3/CD77: Targeting of Gastric Cancer Cells with Shiga Toxin B-Subunit. *Mol Cancer Ther*. 2016;15:1008-17.

Harrus D, Khoder-Agha F, Peltoniemi M, Hassinen A, Ruddock L, Kellokumpu S, Glumoff T. The dimeric structure of wild-type human glycosyltransferase B4GalT1. *PLoS One*. 2018; 13: e0205571.

Jacob F, Anugraham M, Pochechueva T, Tse BW, Alam S, Guertler R, Bovin NV, Fedier A, Hacker NF, Huflejt ME, Packer N, Heinzelmann-Schwarz VA. The glycosphingolipid P_1 is an ovarian cancer-associated carbohydrate antigen involved in migration. *Br J Cancer*. 2014;111:1634-45.

Jayaprakash NG, Surolia A. Role of glycosylation in nucleating protein folding and stability. *Biochem J*. 2017;474:2333-2347.

Jeanneau C, Chazalet V, Augé C, Soumpasis DM, Harduin-Lepers A, Delannoy P, Imberty A, Breton C. Structure-function analysis of the human sialyltransferase ST3Gal I: role of n-glycosylation and a novel conserved sialylmotif. *J Biol Chem*. 2004;279:13461-8.

Johannes L, Römer W. Shiga toxins--from cell biology to biomedical applications. *Nat Rev Microbiol*. 2010; 8: 105-16.

Kaczmarek R, Buczkowska A, Mikołajewicz K, Krotkiewski H, Czerwinski M. P1PK, GLOB, and FORS blood group systems and GLOB collection: biochemical and clinical aspects. Do we understand it all yet? *Transfus Med Rev*. 2014;28:126-36.

Kaczmarek R, Duk M, Szymczak K, Korchagina E, Tyborowska J, Mikolajczyk K, Bovin N, Szewczyk B, Jaskiewicz E, Czerwinski M. Human Gb3/CD77 synthase reveals specificity toward two or four different acceptors depending on amino acid at position 211, creating P(k), P1 and NOR blood group antigens. *Biochem Biophys Res Commun*. 2016;470:168-174.

Kaczmarek R, Mikolajewicz K, Szymczak K, Duk M, Majorczyk E, Krop-Watorek A, Buczkowska A, Czerwinski M. Evaluation of an amino acid residue critical for the specificity and activity of human Gb3/CD77 synthase. *Glycoconj J*. 2016;33:963-973.

Kaczmarek R, Suchanowska A, Lisowska E, Czerwinski M. 2013. Gb3/CD77 synthase (α1,4-galactosyltransferase) and its variant form, NOR-synthase, exist as dimers. Conference: 38th FEBS Congress, St. Petersburg; 07/2012 At: St. Petersburg Volume: 280S1.

Kaczmarek R, Szymczak-Kulus K, Bereźnicka A, Mikołajczyk K, Duk M, Majorczyk E, Krop-Watorek A, Klausa E, Skowrońska J, Michalewska B, Brojer E, Czerwinski M. Single

nucleotide polymorphisms in A4GALT spur extra products of the human Gb3/CD77 synthase and underlie the P1PK blood group system. *PLoS One*. 2018;13:e0196627.

Kato T, Suzuki M, Murata T, Park EY. The effects of N-glycosylation sites and the N-terminal region on the biological function of beta1,3-N-acetylglucosaminyltransferase 2 and its secretion. *Biochem Biophys Res Commun*. 2005;329:699-705.

Kattke MD, Gosschalk JE, Martinez OE, Kumar G, Gale RT, Cascio D, Sawaya MR, Philips M, Brown ED, Clubb RT. Structure and mechanism of TagA, a novel membrane-associated glycosyltransferase that produces wall teichoic acids in pathogenic bacteria. *PLoS Pathog*. 2019;15:e1007723.

Kizuka Y, Kitazume S, Taniguchi N. N-glycan and Alzheimer's disease. *Biochim Biophys Acta Gen Subj*. 2017;1861:2447-2454.

Kovbasnjuk O, Mourtazina R, Baibakov B, Wang T, Elowsky C, Choti MA, Kane A, Donowitz M. The glycosphingolipid globotriaosylceramide in the metastatic transformation of colon cancer. *Proc Natl Acad Sci USA*. 2005;102:19087-92.

Kuśnierz-Alejska G, Duk M, Storry JR, Reid ME, Wiecek B, Seyfried H, Lisowska E. NOR polyagglutination and Sta glycophorin in one family: relation of NOR polyagglutination to terminal alpha-galactose residues and abnormal glycolipids. *Transfusion*. 1999;39:32-8.

Laemmli UK. Cleavage of structural proteins during the assembly of the head of bacteriophage T4. *Nature*. 1970;227:680-5.

Lee MS, Tesh V. Roles of Shiga Toxins in Immunopathology. *Toxins (Basel)*. 2019; 11, 212.

Leong SR, Kabakoff RC, Hébert CA. Complete mutagenesis of the extracellular domain of interleukin-8 (IL-8) type A receptor identifies charged residues mediating IL-8 binding and signal transduction. *J Biol Chem*. 1994;269:19343-8.

Lopez LC, Youakim A, Evans SC, Shur BD. Evidence for a molecular distinction between Golgi and cell surface forms of β1,4-galactosyltransferase. *J. Biol. Chem*. 1991;266:15984-15991.

Lowenthal MS, Davis KS, Formolo T, Kilpatrick LE, Phinney KW. Identification of Novel N-Glycosylation Sites at Noncanonical Protein Consensus Motifs. *J Proteome Res*. 2016;15:2087-101.

Majowicz SE, Scallan E, Jones-Bitton A, Sargeant JM, Stapleton J, Angulo FJ, Yeung DH, Kirk MD. Global incidence of human Shiga toxin-producing Escherichia coli infections and

deaths: a systematic review and knowledge synthesis. *Foodborne Pathog Dis*. 2014;11:447-55.

Martina JA, Daniotti JL, Maccioni HJ. GM1 synthase depends on N-glycosylation for enzyme activity and trafficking to the Golgi complex. *Neurochem Res*. 2000;25:725-31.

Martina JA, Daniotti JL, Maccioni HJ. Influence of N-glycosylation and N-glycan trimming on the activity and intracellular traffic of GD3 synthase. *J Biol Chem*. 1998;273:3725-31.

Maszczak-Seneczko D, Olczak T, Jakimowicz P, Olczak M. Overexpression of UDP-GlcNAc transporter partially corrects galactosylation defect caused by UDP-Gal transporter mutation. *FEBS Lett*. 2011;585, 3090–3094.

Miazek A, Brockhaus M, Langen H, Braun A, Kisielow P. Intrathymic education of alpha beta and gamma delta T cells is accompanied by cell surface expression of RNA/DNA helicase [corrected]. *Eur J Immunol*. 1997;27:3269-82.

Mikolajczyk K, Kaczmarek R, Czerwinski M. How glycosylation affects glycosylation: the role of N-glycans in glycosyltransferase activity. *Glycobiology*. 2020;30:941-969.

Miller JJ, Kanack AJ, Dahms NM. Progress in the understanding and treatment of Fabry disease. *Biochim Biophys Acta Gen Subj*. 2020;1864:129437.

Morimoto K, Suzuki N, Tanida I, Kakuta S, Furuta Y, Uchiyama Y, Hanada K, Suzuki Y, Yamaji T. Blood group P1 antigen-bearing glycoproteins are functional but less efficient receptors of Shiga toxin than conventional glycolipid-based receptors. *J Biol Chem*. 2020;295:9490-9501.

Nagai K, Ihara Y, Wada Y, Taniguchi N. N-glycosylation is requisite for the enzyme activity and Golgi retention of N-acetylglucosaminyltransferase III. *Glycobiology*. 1997;7:769-76.

Nilsson T, Hoe MH, Slusarewicz P, Rabouille C, Watson R, Hunte F, Watzele G, Berger EG, Warren G. Kin recognition between medial Golgi enzymes in HeLa cells. *EMBO J*. 1994; 13: 562-74.

Okuda T, Tokuda N, Numata S, Ito M, Ohta M, Kawamura K, Wiels J, Urano T, Tajima O, Furukawa K, Furukawa K. Targeted disruption of Gb3/CD77 synthase gene resulted in the complete deletion of globo-series glycosphingolipids and loss of sensitivity to verotoxins. *J Biol Chem*. 2006;281:10230-5.

Pagny S, Bouissonnie F, Sarkar M, Follet-Gueye ML, Driouich A, Schachter H, Faye L, Gomord V. Structural requirements for Arabidopsis beta1,2-xylosyltransferase activity and targeting to the Golgi. *Plant J*. 2003;33:189-203.

Patnaik SK, Stanley P. Lectin-resistant CHO glycosylation mutants. *Methods Enzymol*. 2006;416:159-82.

Ramakrishnan B, Qasba PK. Structure-based design of beta 1,4-galactosyltransferase I (beta 4Gal-T1) with equally efficient N-acetylgalactosaminyltransferase activity: point mutation broadens beta 4Gal-T1 donor specificity. *J Biol Chem*. 2002;277:20833-9.

Rosnoblet C, Peanne R, Legrand D, Foulquier F. Glycosylation disorders of membrane trafficking. *Glycoconj J*. 2013;30:23-31.

Ruggiero FM, Vilcaes AA, Iglesias-Bartolomé R, Daniotti JL. Critical role of evolutionarily conserved glycosylation at Asn211 in the intracellular trafficking and activity of sialyltransferase ST3Gal-II. *Biochem J*. 2015;469:83-95.

Ryan SO, Cobb BA. Roles for major histocompatibility complex glycosylation in immune function. *Semin Immunopathol*. 2012;34:425-41.

Sahraneshin Samani F, Moore JK, Khosravani P, Ebrahimi M. Features of free software packages in flow cytometry: a comparison between four non-commercial software sources. *Cytotechnology*. 2014;66:555-9.

Shauchuk A, Szulc B, Maszczak-Seneczko D, Wiertelak W, Skurska E, Olczak M. N-glycosylation of the human β1,4-galactosyltransferase 4 is crucial for its activity and Golgi localization. *Glycoconj J*. 2020;37:577-588.

Simioni P, Tormene D, Tognin G, Gavasso S, Bulato C, Iacobelli NP, Finn JD, Spiezia L, Radu C, Arruda VR. X-linked thrombophilia with a mutant factor IX (factor IX Padua). *N Engl J Med*. 2009;361:1671-5.

Skropeta D. The effect of individual N-glycans on enzyme activity. *Bioorg Med Chem*. 2009;17:2645-53.

Stanley P, Taniguchi N, Aebi M. N-Glycans. 2017. In: Varki A, Cummings RD, Esko JD, Stanley P, Hart GW, Aebi M, Darvill AG, Kinoshita T, Packer NH, Prestegard JH, Schnaar RL, Seeberger PH, editors. Essentials of Glycobiology [Internet]. 3rd ed. Cold Spring Harbor (NY): Cold Spring Harbor Laboratory Press; 2015–2017. Chapter 9.

Stanley P. Selection of lectin-resistant mutants of animal cells. *Methods Enzymol*. 1983;96:157-84.

Stenfelt L, Westman JS, Hellberg Å, Olsson ML. The P1 histo-blood group antigen is present on human red blood cell glycoproteins. *Transfusion*. 2019;59:1108-1117.

Suchanowska A, Kaczmarek R, Duk M, Lukasiewicz J, Smolarek D, Majorczyk E, Jaskiewicz E, Laskowska A, Wasniowska K, Grodecka M, Lisowska E, Czerwinski M. A single point mutation in the gene encoding Gb3/CD77 synthase causes a rare inherited polyagglutination syndrome. *J Biol Chem*. 2012;287:38220-30. Epub 2012 Sep 10. Erratum in: *J Biol Chem*. 2013;288:294.

Szymczak K., Kaczmarek R., Duk M., Mikołajczyk K., Zerka A., Bereznicka A, Olczak M., Czerwinski M. How glycosylation may influence glycosylation: N-glycans of the human alpha1,4 galactosylatransferase (Gb3/CD77 synthase) are crucial for its activity. 2nd Congress BIO2016, Wrocław 13-16.09.2016, *Acta Biochim. Polon*. P22.19.

Szymczak-Kulus K, Mikolajczyk K, Bereznicka A, Lisowska M, Janicka P, Kaczmarek R, Miazek A, Czerwinski M. A new monoclonal antibody recognizing the full-length intracellular human α1,4-galactosyltransferase (Gb3/CD77 synthase) as well as its soluble form in the blood serum. Conference: 29th International Carbohydrate Symposium in 2018 (ICS 2018) At: Lisbon, Portugal.

Szymczak-Kulus K, Weidler S, Bereznicka A, Mikolajczyk K, Kaczmarek R, Olczak M, Park EY, Unverzagt C, Czerwinski M. Novel bisgalactosylated type of N-glycans as decoy receptors for Shiga toxin. 25th International Symposium on Glycoconjugates (Glyco25), Milan, Italy, *Glycoconjugate Journal*, 2019, 36, 267–397.

Taujale R, Venkat A, Huang LC, Zhou Z, Yeung W, Rasheed KM, Li S, Edison AS, Moremen KW, Kannan N. Deep evolutionary analysis reveals the design principles of fold A glycosyltransferases. *Elife*. 2020; 9:e54532.

Towbin H, Staehelin T, Gordon J. Electrophoretic transfer of proteins from polyacrylamide gels to nitrocellulose sheets: procedure and some applications. *Proc Natl Acad Sci USA*. 1979;76:4350-4.

Tuzikov A, Chinarev A, Shilova N, Gordeeva E, Galanina O, Ovchinnikova T, Schaefer M, Bovin N. 40 years of glyco-polyacrylamide in glycobiology. *Glycoconj J*. 2021 [ahead of print].

Uemura S, Kurose T, Suzuki T, Yoshida S, Ito M, Saito M, Horiuchi M, Inagaki F, Igarashi Y, Inokuchi J. Substitution of the N-glycan function in glycosyltransferases by specific amino acids: ST3Gal-V as a model enzyme. *Glycobiology*. 2006;16:258-70.

Vajaria BN, Patel PS. Glycosylation: a hallmark of cancer? *Glycoconj J*. 2017;34:147-156.

Varki A. Biological roles of glycans. *Glycobiology*. 2017;27:3-49.

Wagner GK, Pesnot T, Palcic MM, Jørgensen R. Novel UDP-GalNAc Derivative Structures Provide Insight into the Donor Specificity of Human Blood Group Glycosyltransferase. *J Biol Chem*. 2015;290:31162-72.

Wu W, Xiao L, Wu X, Xie X, Li P, Chen C, Zheng Z, Ai J, Valencia A, Dong B, Ding Q, Dong B, Wang X. Factor IX alteration p.Arg338Gln (FIX Shanghai) potentiates FIX clotting activity and causes thrombosis. *Haematologica*. 2021;106:264-268.

Zhang H, Zhou M, Yang T, Haslam SM, Dell A, Wu H. New Helical Binding Domain Mediates a Glycosyltransferase Activity of a Bifunctional Protein. *J Biol Chem*. 2016;291:22106-22117.

Table 1. **Quantitative analysis of cell surface expression of human Gb3, P1 and NOR antigens in CHO-Lec2 cells transfected with vectors encoding Gb3/CD77 synthase and its mutein glycovariants. A)** Antibody binding capacities (ABC) were calculated using Quantum FITC MESF kit in flow cytometry, by interpolation from calibration curves (median fluorescence intensity versus Molecules of Equivalent Soluble Fluorochrome units) accordingly to the manufacturer's protocol and the fluorophore-to-protein molar ratios of FITC-conjugates. **B)** The order of activity level based on the ABC values measured for Gb3/CD77 synthase and its mutein glycovariants. **C)** The order of *in vitro* activity level measured using PAA-conjugates for Gb3/CD77 synthase and its mutein glycovariants.

A)

Antibody	**Q_{full}**	**Q_{S123A}**	**Q_{T205A}**	**Q_{S123A} / Q_{T205A}**
Anti-P1 (650)	290760 ± 91893	489625 ± 179537	247621 ± 12960	8435 ± 2746
Anti-P1 (P3NIL100)	25135 ± 4623	19531 ± 2839	18649 ± 1401	9513 ± 1126
Anti-NOR (nor118)	-	-	-	-
Antibody	**E_{full}**	**E_{S123A}**	**E_{T205A}**	**E_{S123A} / E_{T205A}**
Anti-P1 (650)	713763 ± 44309	520503 ± 40406	140609 ± 1427	3724 ± 1281
Anti-P1 (P3NIL100)	36684 ± 6760	15772 ± 2013	19333 ± 1532	657 ± 285
Anti-NOR (nor118)	84710 ± 13952	186243 ± 9443	40164 ± 1989	1127 ± 52

B)

Anti-P1 (650)	
Gb3/CD77 synthase	**Mutein**
$Q_{S123A} > Q_{full} > Q_{T205A} > Q_{S123A} / Q_{T205A}$	$E_{full} > E_{S123A} > E_{T205A} > E_{S123A} / E_{T205A}$
Anti-P1 (P3NIL100)	
Gb3/CD77 synthase	**Mutein**
$Q_{full} > Q_{S123A} > Q_{T205A} > Q_{S123A} / Q_{T205A}$	$E_{full} > E_{T205A} > E_{S123A} > E_{S123A} / E_{T205A}$
Anti-NOR (nor118)	
Gb3/CD77 synthase	**Mutein**
-	$E_{S123A} > E_{full} > E_{T205A} > E_{S123A} / E_{T205A}$

C)

Anti-P1 (650)	
Gb3/CD77 synthase	**Mutein**
$Q_{full} > Q_{S123A} > Q_{T205A} > Q_{S123A} / Q_{T205A}$	$E_{full} > E_{S123A} > E_{T205A} > E_{S123A} / E_{T205A}$
Anti-P1 (P3NIL100)	
Gb3/CD77 synthase	**Mutein**
$Q_{full} = Q_{S123A} > Q_{T205A} > Q_{S123A} / Q_{T205A}$	$E_{full} > E_{S123A} > E_{T205A} > E_{S123A} / E_{T205A}$
Anti-NOR (nor118)	
Gb3/CD77 synthase	**Mutein**
-	$E_{S123A} > E_{full} > E_{T205A} > E_{S123A} / E_{T205A}$

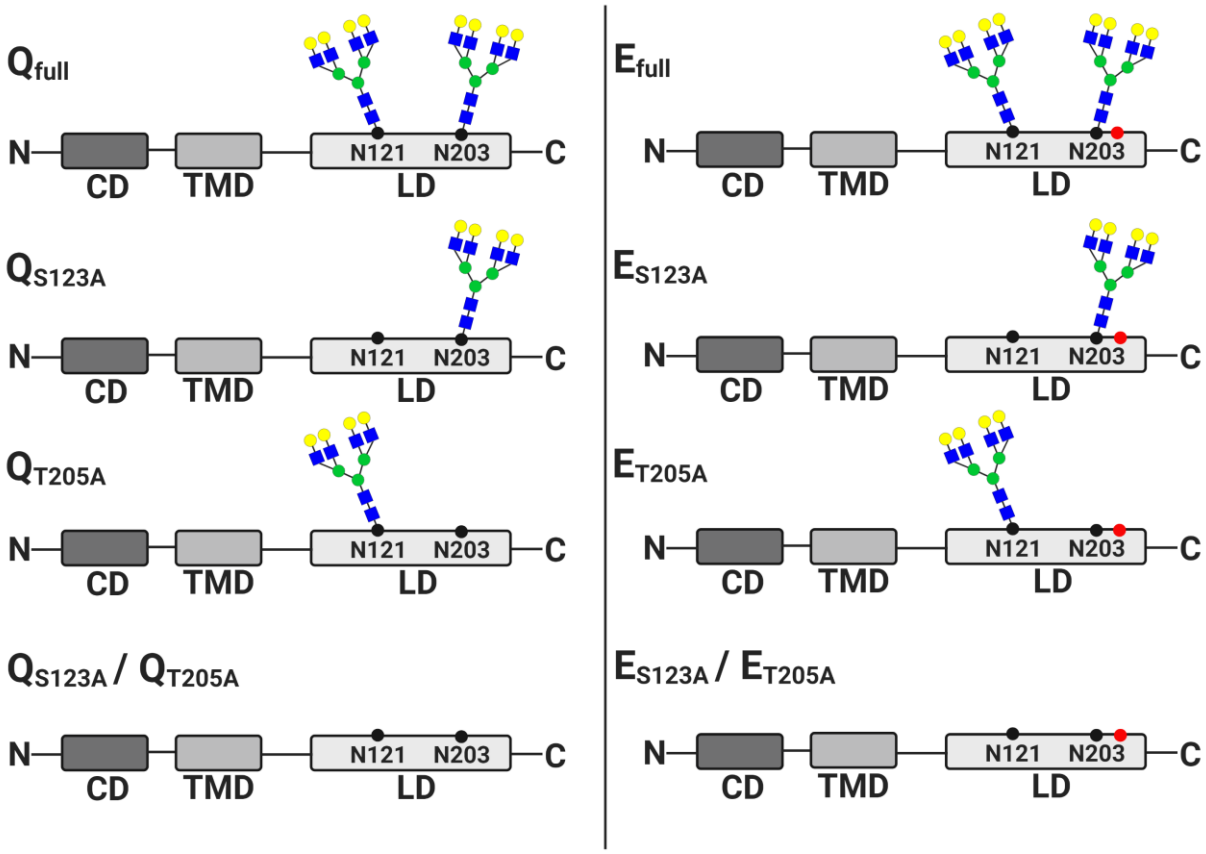

Fig. 1. **Schematic representation of human Gb3/CD77 synthase and its mutein glycovariants with N-glycosylation sites occupation.** The enzyme contains cytoplasmic domain (CD, encompasses 1-22 amino acids residues), transmembrane domain (TMD, encompasses 23-43 amino acids residues) which resides the enzyme in Golgi apparatus membrane and lumenal domain (LD, encompasses 44-353 amino acids residues), containing catalytic site. The sequences of human Gb3/CD77 synthase domains according with UniProt (Q9NPC4, https://www.uniprot.org/). The Gb3/CD77 synthase in contrast to its mutein with p.Q211E substitution (red dot). Both Gb3/CD77 synthase forms contain two N-glycosylation sites at N_{121} and N_{203}. Q_{full}, fully N-glycosylated of Gb3/CD77 synthase; E_{full}, fully N-glycosylated mutein Gb3/CD77 synthase; Q_{S123A}, Gb3/CD77 synthase with p.S123A substitution; E_{S123A}, mutein Gb3/CD77 synthase with p.S123A substitution; Q_{T205A}, Gb3/CD77 synthase with p.T205A substitution; E_{T205A}, mutein Gb3/CD77 synthase with p.T205A substitution; Q_{S123A}/Q_{T205A}, Gb3/CD77 synthase with p.S123A/p.T205A substitutions; E_{S123A}/E_{T205A}, mutein Gb3/CD77 synthase with p.S123A/p.T205A substitutions.

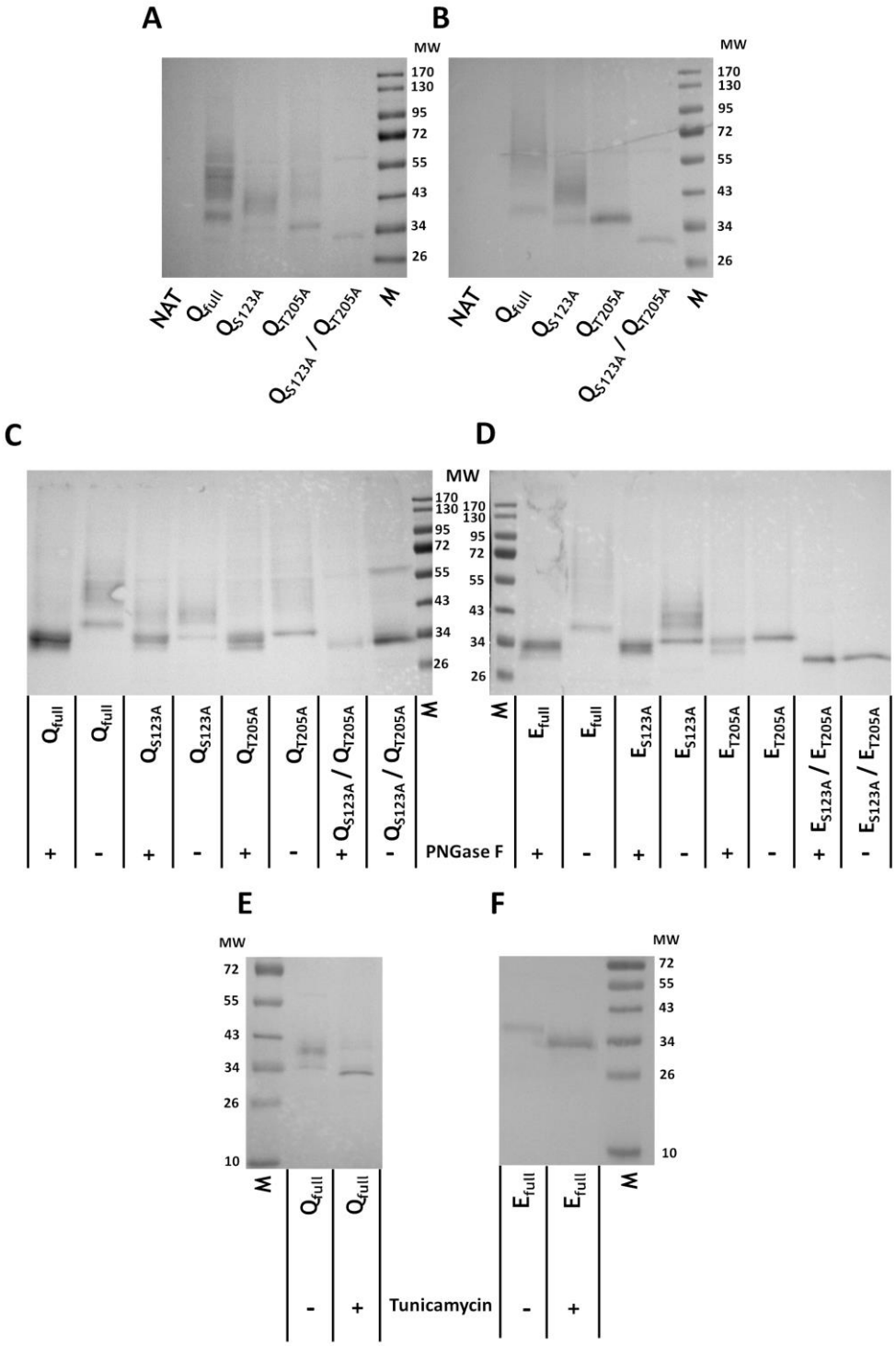

Fig. 2. **Glycosylation patterns of human Gb3/CD77 synthase and its mutein glycovariants.** Western blotting analysis of lysates prepared from CHO-Lec2 cells expressed full N-glycosylated enzymes (Q_{full}, E_{full}) as well as Q_{S123A}, E_{S123A}, Q_{T205A}, E_{T205A}, Q_{S123A}/Q_{T205A} and E_{S123A}/E_{T205A} glycovariants. Human Gb3/CD77 synthase was stained using anti-A4GALT antibody (5C7 culture supernatant). Evaluating molecular weight of (**A**) human Gb3/CD77 synthase its (**B**) mutein glycovariants. (**C**) Human Gb3/CD77 synthase and its (**D**) mutein glycovariants treated (+) or not (-) with PNGase F. CHO-Lec2 cells transfected with vector encoding (**E**) Q_{full} and (**F**) E_{full} were treated (+) or not (-) with tunicamycin. Molecular weight of the bands are presented as a kDa.

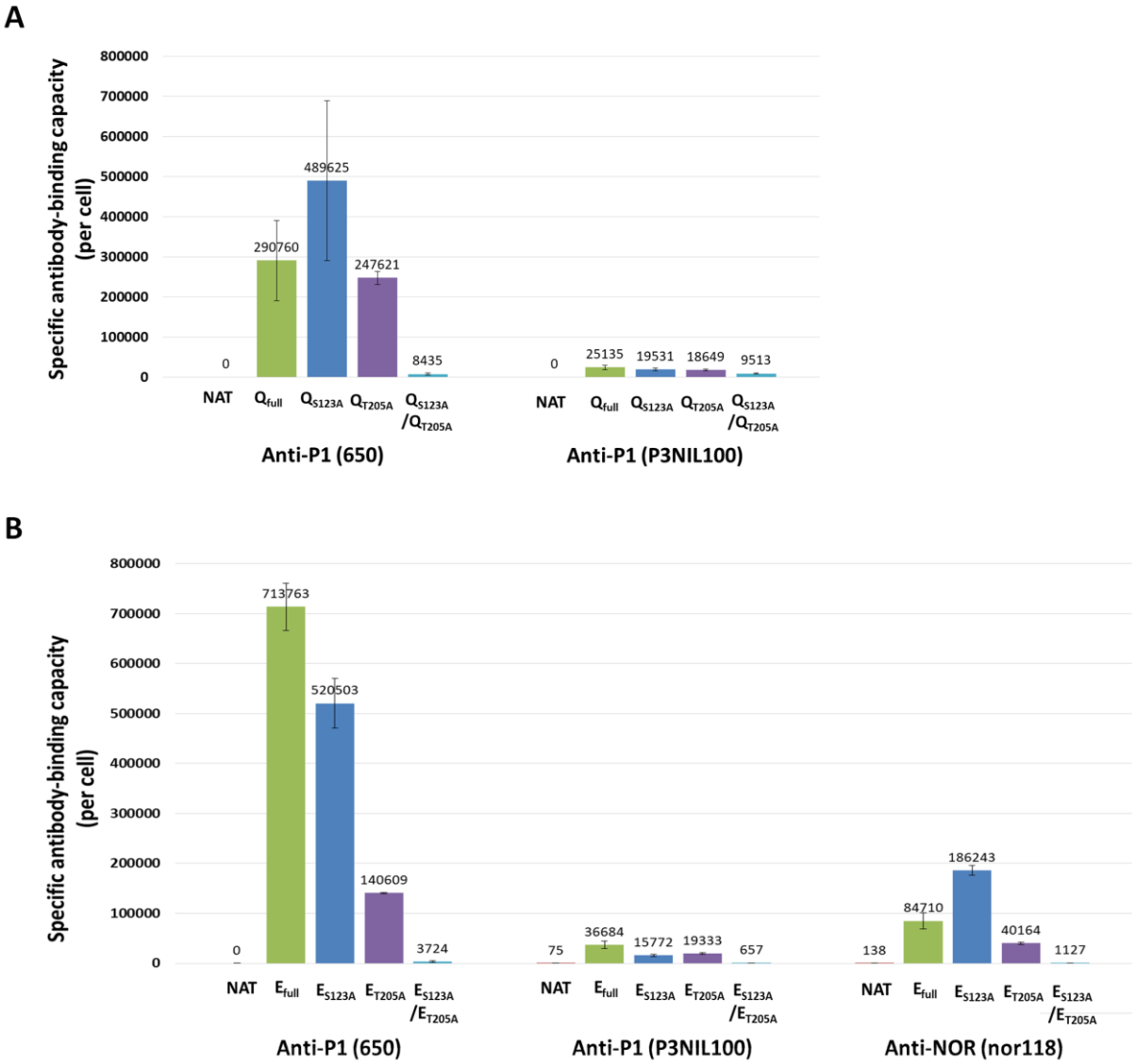

Fig. 3. **Quantitative flow cytometry of Gb3, P1 and NOR antigens expressing on CHO-Lec2 cells**. Antigen binding capacity (ABC) was calculated for anti-P1 (clones 650 and P3NIL100) antibodies and anti-NOR (nor118) antibody binding capacity per CHO-Lec2 cell. (**A**) Human Gb3/CD77 and its (**B**) mutein glycovariants. (median; error bars error bars represent interquartile ranges). Q_{full}, fully N-glycosylated of Gb3/CD77 synthase; E_{full}, fully N-glycosylated mutein Gb3/CD77 synthase; Q_{S123A}, Gb3/CD77 synthase with p.S123A substitution; E_{S123A}, mutein Gb3/CD77 synthase with p.S123A substitution; Q_{T205A}, Gb3/CD77 synthase with p.T205A substitution; E_{T205A}, mutein Gb3/CD77 synthase with p.T205A substitution; Q_{S123A}/Q_{T205A}, Gb3/CD77 synthase with p.S123A/p.T205A substitutions; E_{S123A}/E_{T205A}, mutein Gb3/CD77 synthase with p.S123A/p.T205A substitutions.

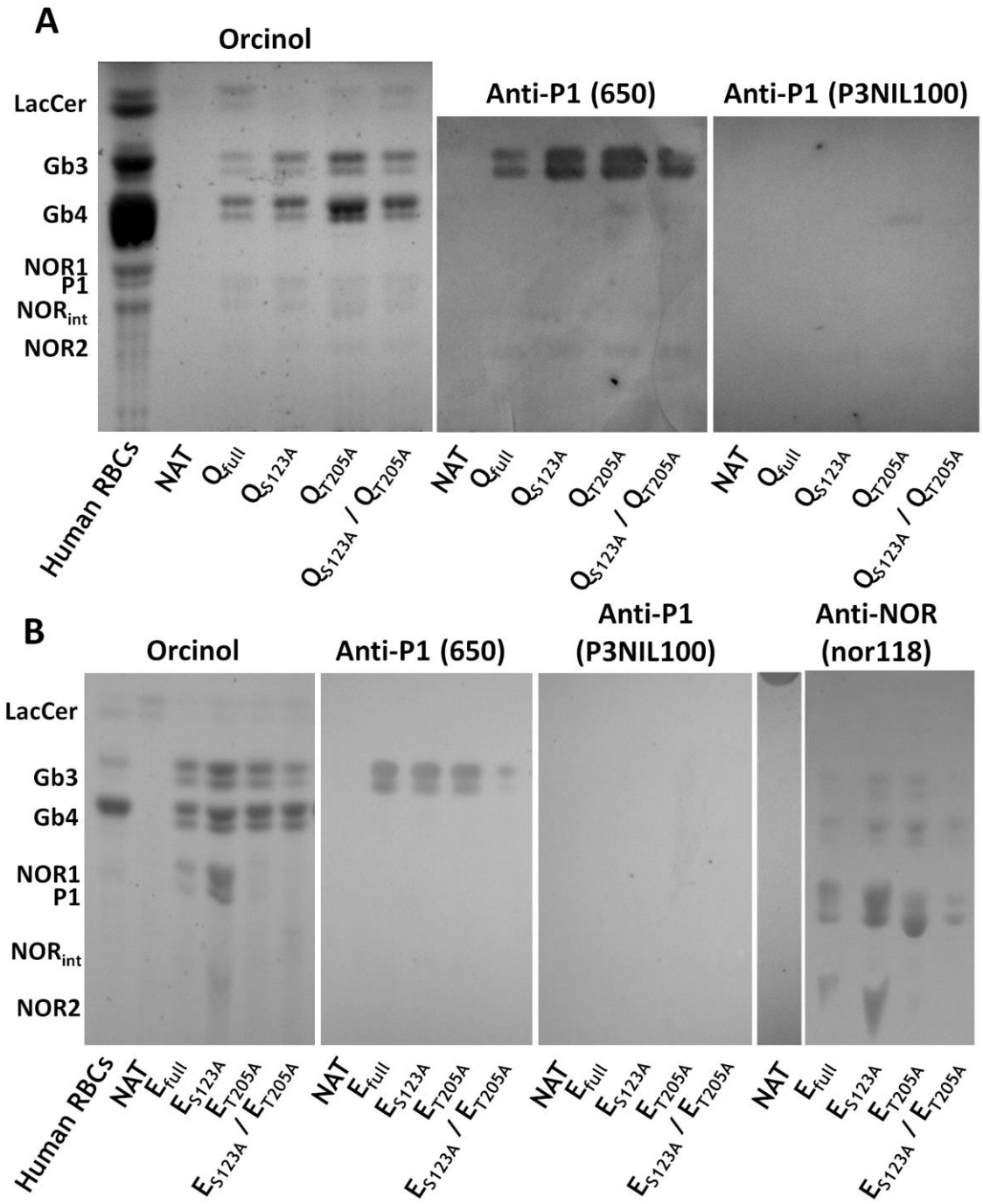

Fig. 4. **HPTLC analysis of neutral glycosphingolipids extracted from CHO-Lec2 cells expressing human Gb3/CD77 synthase and its mutein glycovariants**. (**A**) Gb3/CD77 synthase and its (**B**) mutein glycovariants analyzed by orcinol staining or by overlaying with anti-P1 (650 and P3NIL100) antibodies and anti-NOR (nor118) antibody. Human RBCs, the GSLs samples of $P^{1NOR}P^{1}$ human RBCs; NAT, untransfected CHO-Lec2 cells; Q_{full}, fully N-glycosylated of Gb3/CD77 synthase; E_{full}, fully N-glycosylated mutein Gb3/CD77 synthase; Q_{S123A}, Gb3/CD77 synthase with p.S123A substitution; E_{S123A}, mutein Gb3/CD77 synthase with p.S123A substitution; Q_{T205A}, Gb3/CD77 synthase with p.T205A substitution; E_{T205A}, mutein Gb3/CD77 synthase with p.T205A substitution; Q_{S123A}/Q_{T205A}, Gb3/CD77 synthase with p.S123A/p.T205A substitutions; E_{S123A}/E_{T205A}, mutein Gb3/CD77 synthase with p.S123A/p.T205A substitutions.

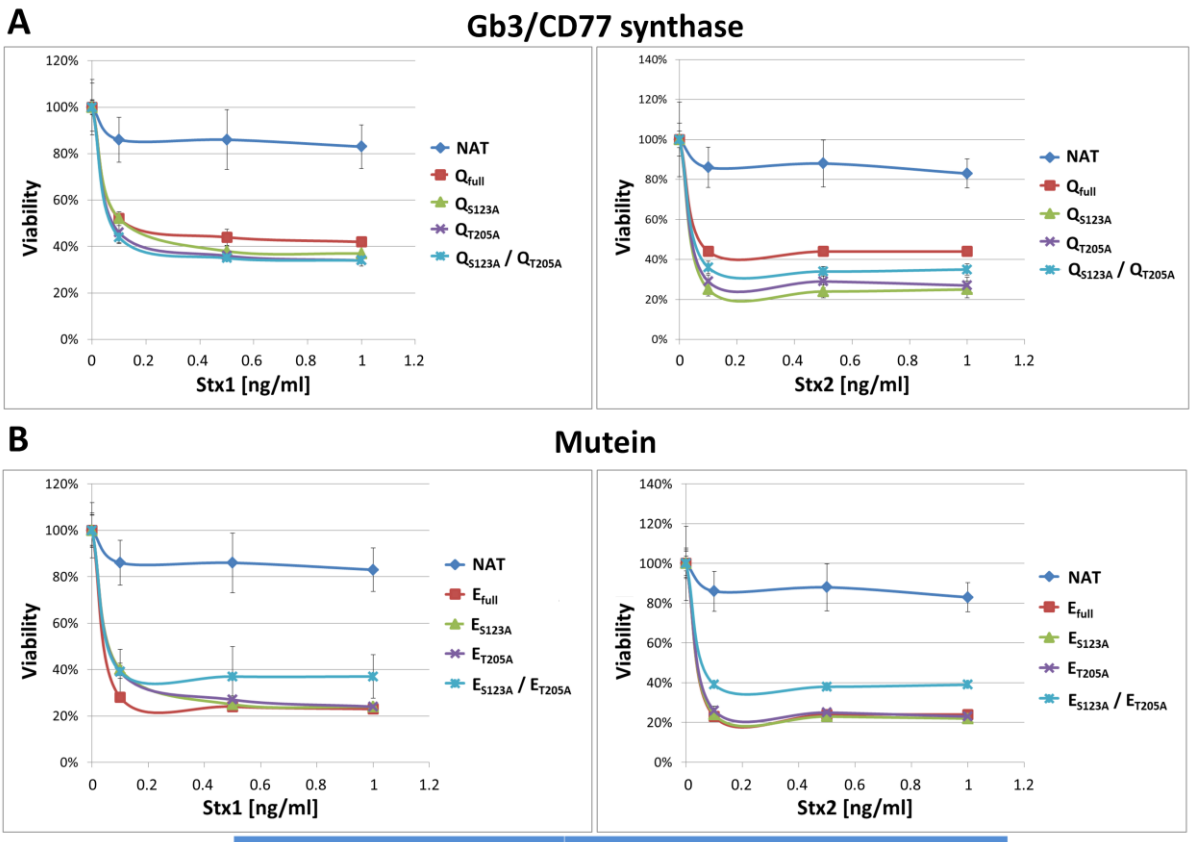

Enzyme	p value for different Stx concentration (Kruskal-Wallis ANOVA test by ranks)	
	Stx1	Stx2
NAT	0.9439	0.7220
Q_{full}	0.0003	0.0040
E_{full}	0.0002	0.0042
Q_{S123A}	0.0011	0.0041
E_{S123A}	0.0010	0.0059
Q_{T205A}	0.0009	0.0089
E_{T205A}	0.0007	0.0036
Q_{S123A}/Q_{T205A}	0.0011	0.0067
E_{S123A}/E_{T205A}	0.0007	0.0056

Fig. 5. **Shiga toxins cytotoxicity analysis**. Viability of CHO-Lec2 cells transfected with genes encoding (**A**) Gb3/CD77 synthase and its (**B**) mutein glycovariants treated with Stx1 and Stx2 holotoxins were evaluated (at least three independent experiments were conducted, each with three technical replicates; error bars are standard deviations). Tables contain p values of the Kruskal-Wallis ANOVA test (statistical significance when $p < 0.05$). Q_{full}, fully N-glycosylated of Gb3/CD77 synthase; E_{full}, fully N-glycosylated mutein Gb3/CD77 synthase; Q_{S123A}, Gb3/CD77 synthase with p.S123A substitution; E_{S123A}, mutein Gb3/CD77 synthase with p.S123A substitution; Q_{T205A}, Gb3/CD77 synthase with p.T205A substitution; E_{T205A}, mutein Gb3/CD77 synthase with p.T205A substitution; Q_{S123A}/Q_{T205A}, Gb3/CD77 synthase with p.S123A/p.T205A substitutions; E_{S123A}/E_{T205A}, mutein Gb3/CD77 synthase with p.S123A/p.T205A substitutions.

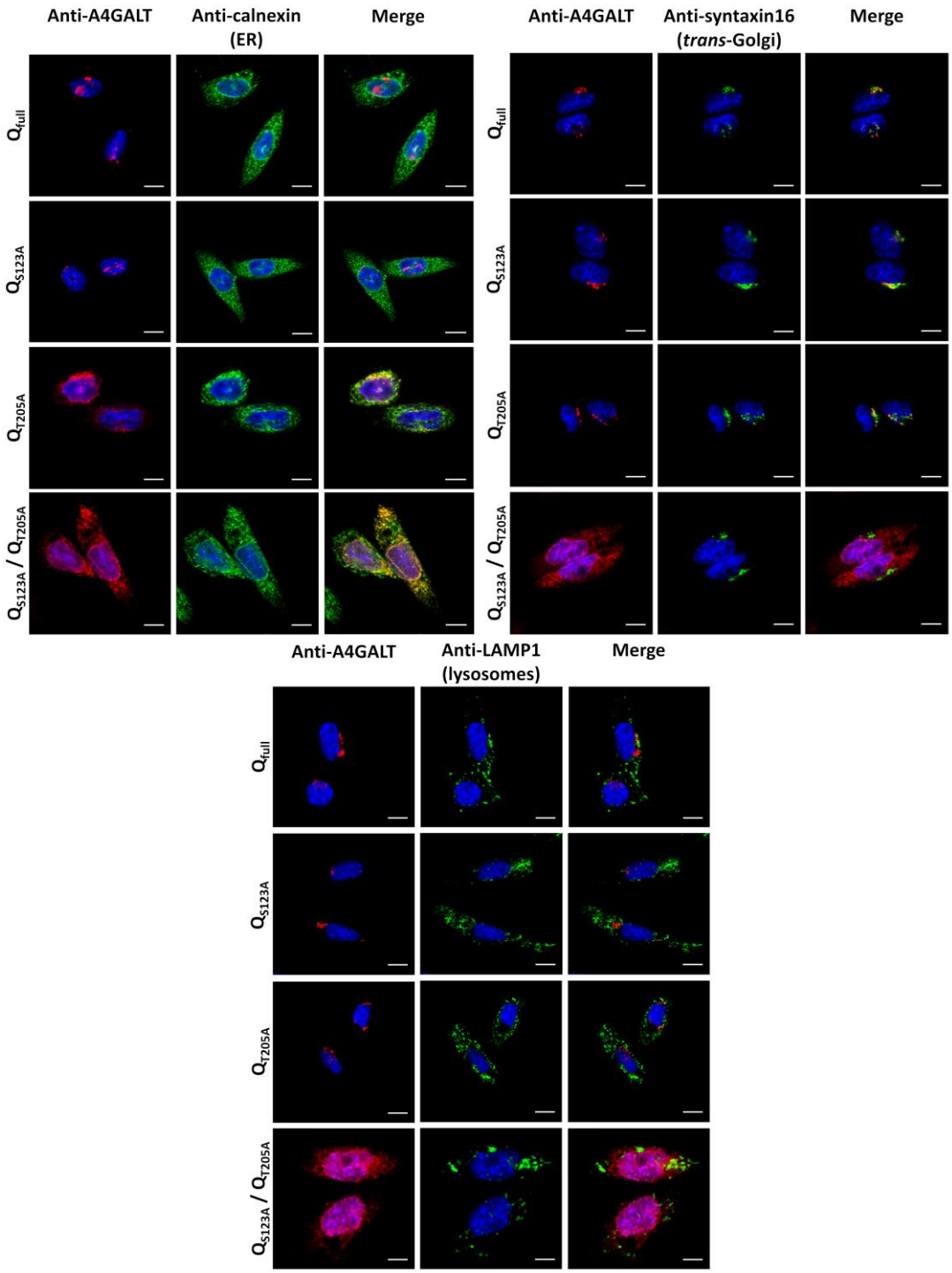

Fig. 6. **Subcellular localization of human Gb3/CD77 synthase glycovariants in CHO-Lec2 cells using immunofluorescence**. Human Gb3/CD77 synthase glycovariants expressed in CHO-Lec2 cells were visulized using anti-A4GALT (5C7 culture supernatant) antibody (red). The cellular organelles, such as Golgi apparatus, endoplasmic reticulum and lysosomes and early endosomes were immunostained by specific antibody recognizing organellum-specific marker (green). Cell nuclei were counterstained with DAPI (blue). Q_{full}, fully N-glycosylated of Gb3/CD77 synthase; Q_{S123A}, Gb3/CD77 synthase with p.S123A substitution; Q_{T205A}, Gb3/CD77 synthase with p.T205A substitution; Q_{S123A}/Q_{T205A}, Gb3/CD77 synthase with p.S123A/p.T205A substitutions. Scale bar −10 μm.

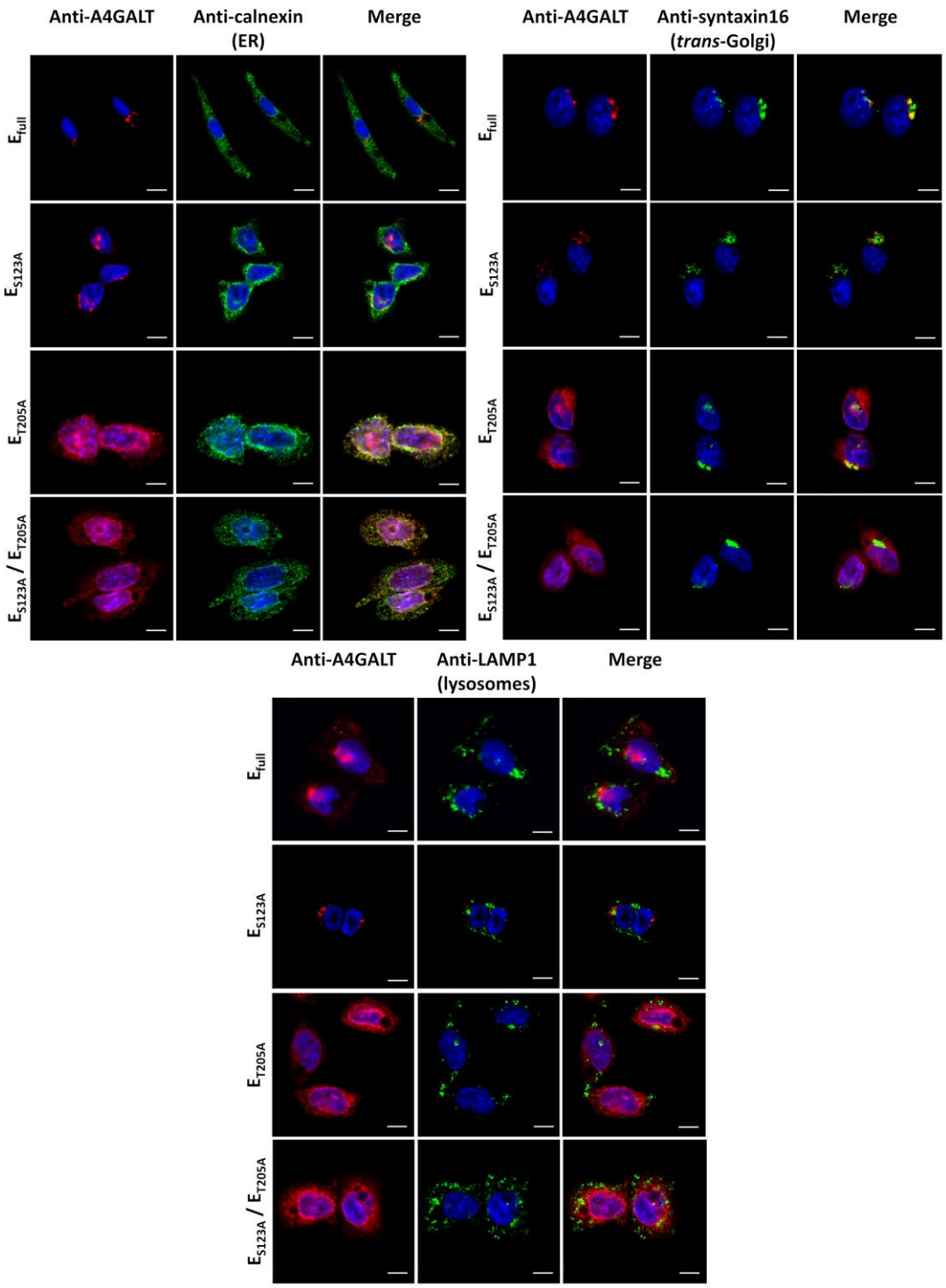

Fig. 7. **Subcellular localization of mutein glycovariants in CHO-Lec2 cells using immunofluorescence**. Mutein glycovariants expressed in CHO-Lec2 cells were visulized using anti-A4GALT (5C7 culture supernatant) antibody (red). The cellular organelles, such as Golgi apparatus, endoplasmic reticulum and lysosomes and early endosomes were immunostained by specific antibody recognizing organellum-specific marker (green). Cell nuclei were counterstained with DAPI (blue). E_{full}, fully N-glycosylated mutein Gb3/CD77 synthase; E_{S123A}, mutein Gb3/CD77 synthase with p.S123A substitution; E_{T205A}, mutein Gb3/CD77 synthase with p.T205A substitution; E_{S123A}/E_{T205A}, mutein Gb3/CD77 synthase with p.S123A/p.T205A substitutions. Scale bar −10 μm.